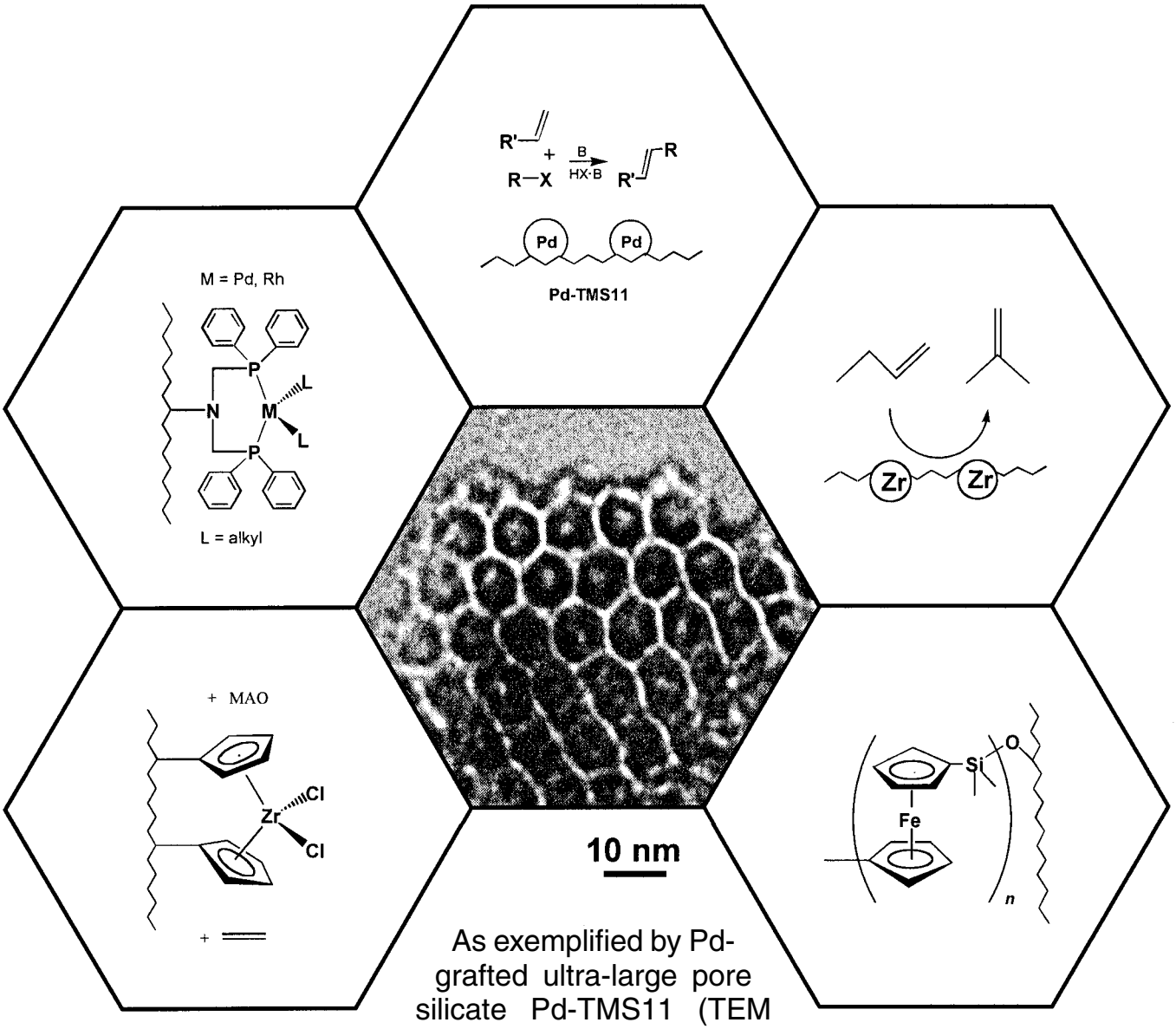

As exemplified by Pd-grafted ultra-large pore silicate Pd-TMS11 (TEM image presented above), supramolecular-templated mesoporous materials find many uses, for example (starting at the left and going clockwise) in polymerization, for immobilization of well-defined homogeneous catalysts, in Heck catalysis, in acid catalysis, and as an encapsulation host for ferrocenyl units.

Synthesis and Applications of Supramolecular-Templated Mesoporous Materials**

Jackie Y. Ying,* Christian P. Mehnert, and Michael S. Wong

Research in supramolecular-templated mesoporous materials began in the early 1990s with the announcement of MCM-41 and the M41S family of molecular sieves. These materials are highly unusual in their textural characteristics: uniform pore sizes greater than 20 Å, surface areas in excess of 1000 $m^2 g^{-1}$, and long-range ordering of the packing of pores. The mesoporous materials are derived with supramolecular assemblies of surfactants, which template the inorganic components during synthesis. Many researchers have since exploited this technique of supramolecular templating to produce materials with different compositions, new pore systems, and novel properties. This article reviews the current state of the art in mesoporous materials research in three general areas: synthesis, catalytic properties, and other applications that take advantage of bulk morphologies. Various mechanisms formulated to explain the formation of mesostructures are discussed in the context of compositional control. The catalytic applications of mesoporous materials are examined, with a significant fraction based on recent patent literature. Other directions in the utilization of mesoporous materials are also presented.

Keywords: amphiphiles · heterogeneous catalysis · mesoporosity · molecular sieves · template synthesis

1. Introduction

Only six years have passed since the exciting discovery of the novel family of molecular sieves called M41S was reported by the researchers at Mobil Research and Development Corporation.[1] These mesoporous (alumino)silicate materials, with well-defined pore sizes of 15–100 Å, break past the pore-size constraint (< 15 Å) of microporous zeolites. The extremely high surface areas (> 1000 $m^2 g^{-1}$) and the precise tuning of pore sizes are among the many desirable properties that have made such materials the focus of great interest. The M41S materials also ushered in a new approach in materials synthesis where, instead of the use of single molecules as templating agents (as in the case of zeolites), self-assembled molecular aggregates or supramolecular assemblies are employed as the structure-directing agents. Various aspects of M41S and related mesoporous materials have been reviewed by Brinker (recent advances in porous inorganic materials),[2] Vartuli et al. (synthesis of the M41S family),[3] Stucky et al. (biomimetic synthesis of mesoporous materials),[4] Raman et al. (porous silicates templated by surfactants and organosilicate precursors),[5] Antonelli and Ying (mesoporous transition metal oxide (TMS) family),[6] Behrens (mesoporous transition metal oxides),[7] Zhao et al. (aluminosilicate MCM-41),[8] and Sayari (catalytic applications of MCM-41).[9] Here we review the current state of mesoporous materials research from the standpoint of compositional control. The synthesis of not only (alumino)silicate M41S materials but also transition metal doped and pure transition metal oxide mesoporous materials is addressed. After discussion of the major synthesis routes and mechanisms of formation, the applications of these materials are surveyed, with particular emphasis on heterogeneous catalysis.

Inorganic solids that contain pores with diameters in the size range of 20–500 Å are considered mesoporous materials, according to IUPAC definition. Examples of mesoporous materials include M41S, aerogels, and pillared layered structures, as listed in Table 1.[10] In this paper, we will focus only on "mesoporous materials" that have been prepared by supramolecular templating, such as M41S. The demarcation at 20 Å between the micropore and mesopore regimes is convenient, in that all zeolites and related zeotypes are microporous; however, some types of the supramolecular-templated structures can be microporous (see Section 2.4). Mesoporous materials derived by means of surfactant templating are occasionally called "zeolites" and described as "crystalline" materials in reference to their long-range ordering of the pore packing. Such references are not correct, as the pore walls of these materials are amorphous and lack long-range order.

[*] Prof. J. Y. Ying, Dr. C. P. Mehnert, M. S. Wong
Department of Chemical Engineering
Massachusetts Institute of Technology
Cambridge, MA 02139 (USA)
Fax: (+1) 617-258-5766
E-mail: jyying@mit.edu

[**] A list of abbreviations is provided in the Appendix.

  1433-7851/99/3801-0057 $ 17.50+.50/0

Table 1. Pore-size regimes and representative porous inorganic materials.

Pore-size regimes	Definition	Examples	Actual size range
macroporous	> 500 Å	glasses	> 500 Å
mesoporous	20 – 500 Å	aerogels	> 100 Å
		pillared layered clays	10 Å, 100 Å[a]
		M41S	16 – 100 Å
microporous	< 20 Å	zeolites, zeotypes	< 14.2 Å
		activated carbon	6 Å

[a] Bimodal pore-size distribution.

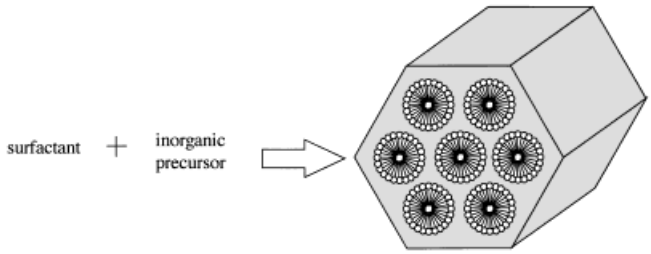

Scheme 1. Schematic representation of the general formation of MCM-41 from inorganic precursors and organic surfactants.

2. Mechanisms of Mesostructure Formation

There have been a number of models proposed to explain the formation of mesoporous materials and to provide a rational basis for the various synthesis routes. On the most common level, these models are predicated upon the presence of surfactants in a solution to guide the formation of the inorganic mesostructure from the solubilized inorganic precursors (Scheme 1). Surfactants contain a hydrophilic head group and a long hydrophobic tail group within the same molecule and will self-organize in such a way as to minimize contact between the incompatible ends. How the inorganic precursor interacts with the surfactant is the issue whereby the models diverge; the type of interaction between the surfactant and the inorganic precursor will be seen as a significant difference among the various synthesis routes, the formation models, and the resulting classes of mesoporous materials.

J. Y. Ying

C. P. Mehnert

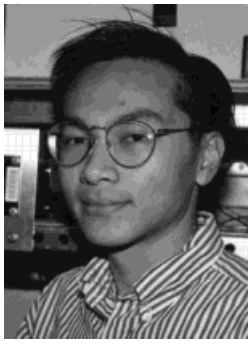

M. S. Wong

Jackie Y. Ying was born in Taiwan and raised in Singapore. She graduated summa cum laude from The Cooper Union in 1987, and completed her Ph.D. degree as an AT&T Bell Laboratories Scholar at Princeton University in 1991. She was a NSF-NATO Postdoctoral Fellow and Alexander von Humboldt Research Fellow at the University of Saarland with Prof. H. Gleiter, and she currently holds the St. Laurent Associate Professorship at the Chemical Engineering Department of the Massachusetts Institute of Technology. Her research is focused on the synthesis of nanostructured inorganic materials for catalytic, membrane, and advanced ceramic applications. She is the author of over eighty publications, and the recipient of the American Ceramic Society Ross C. Purdy Award, David and Lucile Packard Fellowship, National Science Foundation and Office of Naval Research Young Investigator Awards, Camille Dreyfus Teacher-Scholar Award, Royal Academy of Engineering ICI Faculty Fellowship, and American Chemical Society Faculty Fellowship Award in Solid-State Chemistry. She serves on the Board of Directors of the Alexander von Humboldt Association of America as well as the editorial boards of several journals.

Christian P. Mehnert studied chemistry at the Technische Universität München (1985 – 1992). During this time he carried out research with Dr. D. O'Hare at Oxford University (1990) and Prof. J. Lewis at Cambridge University (1991), before he completed his research thesis which focused on the synthesis of new aminocarbyne complexes of chromium with Prof. W. A. Herrmann and Prof. A. C. Filippou (1992). He then moved to England, where he became a graduate student at Oxford University with Prof. M. L. H. Green to work on the synthesis of new organometallic complexes with metal vapor synthesis techniques and the investigation of the reaction chemistry of highly Lewis acidic perfluorinated borane complexes. After receiving his doctorate (D.Phil.) as a student at Balliol College (1996), he moved to the United States and joined Prof. J. Y. Ying's laboratory at the Massachusetts Institute of Technology as a postdoctoral research associate. The area of his current research is the synthesis and application of new nanostructured materials for catalysis, with a special focus on the incorporation of organometallic catalysts into mesoporous molecular sieves.

Michael S. Wong is a Ph.D. student in Chemical Engineering at the Massachusetts Institute of Technology. He received a B.S. degree in Chemical Engineering from the California Institute of Technology (1990 – 1994) and a M.S. degree in Chemical Engineering Practice from the Massachusetts Institute of Technology (1997). His research interests include the synthesis and characterization of nanostructured zirconia-based material for acid catalytic applications.

2.1. Pure Silicate Composition

2.1.1. Liquid Crystal Templating Mechanism

The original M41S family of mesoporous molecular sieves was synthesized, in general, by the combination of appropriate amounts of a silica source (e.g. tetraethylorthosilicate (TEOS), Ludox, fumed silica, sodium silicate), an alkyltrimethylammonium halide surfactant (e.g. cetyltrimethylammonium bromide (CTAB)), a base (e.g. sodium hydroxide or tetramethylammonium hydroxide (TMAOH)), and water. Aluminosilicate M41S was synthesized by the addition of an aluminum source to the synthesis mixture. The mixture was aged at elevated temperatures ($\geq 100\,^{\circ}C$) for 24 to 144 hours, which resulted in a solid precipitate. The organic–inorganic mesostructured product was filtered, washed with water, and air-dried. The product was calcined at about 500 °C under a flowing gas to burn off the surfactant, to yield the mesoporous material.

A "liquid crystal templating" (LCT) mechanism was proposed by the Mobil researchers, based on the similarity between liquid crystalline surfactant assemblies (i.e., lyotropic phases) and M41S.[1] The common traits were the mesostructure dependence on the hydrocarbon chain length of the surfactant tail group,[11] the effect of variation of the surfactant concentrations, and the influence of organic swelling agents. With MCM-41 (which has hexagonally packed cylindrical mesopores) as the representative M41S material, two mechanistic pathways were postulated by the Mobil researchers (Scheme 2):

1) The aluminosilicate precursor species occupied the space between a preexisting hexagonal lyotropic liquid crystal (LC) phase and deposited on the micellar rods of the LC phase.
2) The inorganics mediated, in some manner, the ordering of the surfactants into the hexagonal arrangement.

In either case, the inorganic components (which were negatively charged at the high pH values used) preferentially interacted with the positively charged ammonium head groups of the surfactants and condensed into a solid, continuous framework. The resulting organic–inorganic mesostructure could be alternatively viewed as a hexagonal array of surfactant micellar rods embedded in a silica matrix; removal of the surfactants produced the open, mesoporous MCM-41 framework. It is now known that pathway 1 did not take place because the surfactant concentrations used were far below the critical micelle concentration (CMC) required for hexagonal LC formation.[12] This mechanistic pathway was shown possible recently under different synthesis conditions (see Section 2.1.5).

The second mechanistic pathway of LCT was vaguely postulated as a cooperative self-assembly of the ammonium surfactant and the silicate precursor species below the CMC. It has been known that no preformed LC phase was necessary for MCM-41 formation but, to date, the actual details of MCM-41 formation have not yet been fully agreed upon. Several mechanistic models have been advanced which share the basic idea that the silicate species promoted LC phase formation below the CMC.

2.1.1.1. Silicate Rod Assembly

Davis and co-workers[13] found that the hexagonal LC phase did not develop during MCM-41 synthesis, based on in situ ^{14}N NMR spectroscopy. They proposed that, under the synthesis conditions reported by Mobil, the formation of MCM-41 began with the deposition of two to three monolayers of silicate precursor onto isolated surfactant micellar rods (Scheme 3). The silicate-encapsulated rods were randomly

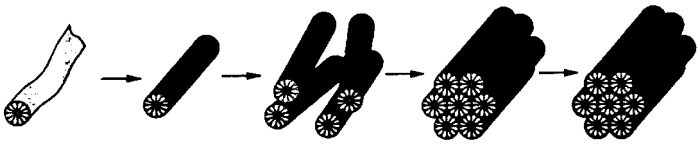

Scheme 3. Assembly of silicate-encapsulated rods (adapted from ref. [13]).

ordered, eventually packing into a hexagonal mesostructure. Heating and aging then completed the condensation of the silicates into the as-synthesized MCM-41 mesostructure.

2.1.1.2. Silicate Layer Puckering

Instead of the formation of silicate-covered micellar rods, Steel et al.[14] postulated that surfactant molecules assembled directly into the hexagonal LC phase upon addition of the silicate species, based on ^{14}N NMR spectroscopy. The silicates were organized into layers, with rows of the cylindrical rods intercalated between the layers (Scheme 4). Aging the

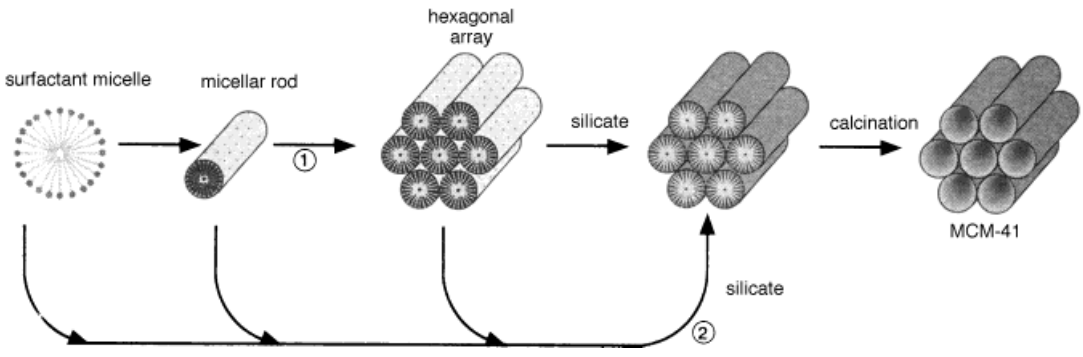

Scheme 2. Two possible pathways for the LCT mechanism.[1b]

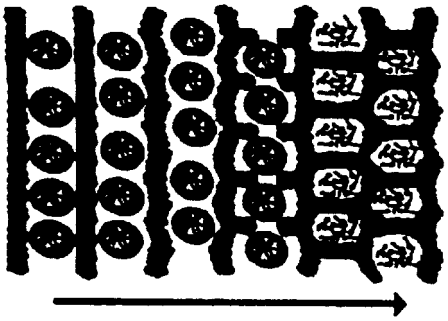

Scheme 4. Puckering of silicate layers in the direction shown (adapted from ref. [14]).

mixture caused the layers to pucker and collapse around the rods, which then transformed into the surfactant-containing MCM-41 hexagonal-phase mesostructure.

2.1.1.3. "Charge Density Matching"

A "charge density matching" mechanistic model was proposed by Monnier et al.[15] and Stucky et al.[16] and suggested that MCM-41 could be derived from a lamellar phase. The initial phase of the synthesis mixture was layered (as detected by X-ray diffractometry (XRD)), and was formed from the electrostatic attraction between the anionic silicates and the cationic surfactant head groups (Scheme 5).

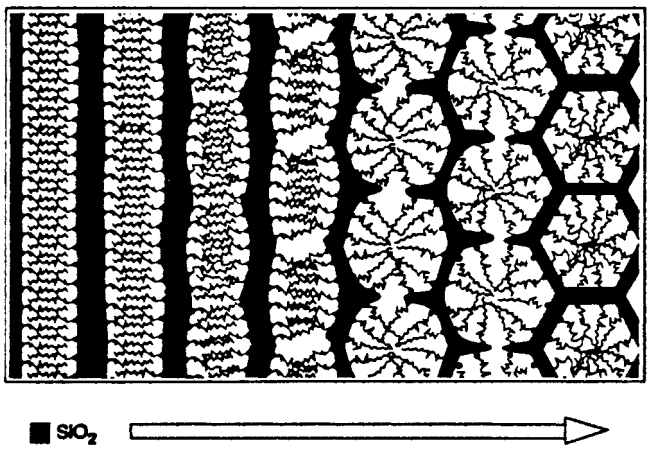

Scheme 5. Curvature induced by charge density matching.[15] The arrow indicates the reaction coordinate.

As the silicate species began to condense, the charge density was reduced. Accompanying this process, curvature was introduced into the layers to maintain the charge density balance with the surfactant head groups, which transformed the lamellar mesostructure into the hexagonal mesostructure.

2.1.1.4. "Folding Sheets"

The lamellar-to-hexagonal phase motif also appeared in materials called FSM prepared from the intercalation of the ammonium surfactant in kanemite, a type of hydrated sodium silicate composed of single-layered silica sheets.[17] After the surfactants were ion-exchanged into the layered structure, the silicate sheets were thought to fold around the surfactants and condense into a hexagonal mesostructure (Scheme 6). The

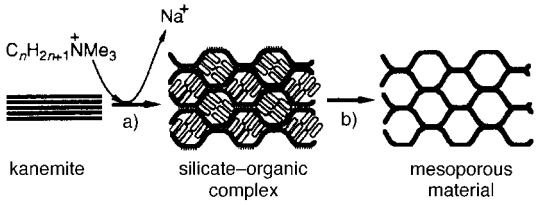

Scheme 6. Folding of silicate sheets around intercalated surfactant molecules.[17b] a) Ion exchange, b) calcination.

final product was claimed to be very similar to MCM-41, with no resemblance to the original kanemite structure. However, Vartuli et al.[12] found that the layered structures were still retained in the kanemite-derived mesoporous materials.

2.1.1.5. "Silicatropic Liquid Crystals"

Under synthesis conditions that prevented condensation of the silicate species, such as low temperatures and high pH ($\approx$14), a true cooperative self-assembly of the silicates and surfactants was found possible. Firouzi et al.[18] conclusively showed, through ^{2}H and ^{29}Si NMR spectroscopy, and neutron scattering, that a micellar solution of CTAB transformed to a hexagonal phase in the presence of silicate anions; this was consistent with the effect of electrolytes on micellar phase transitions.[19] The silicate anions ion-exchanged with the surfactant halide counterions, to form a "silicatropic liquid crystal" (SLC) phase that involved silicate-encrusted cylindrical micelles (Scheme 7). The SLC phase exhibited behavior

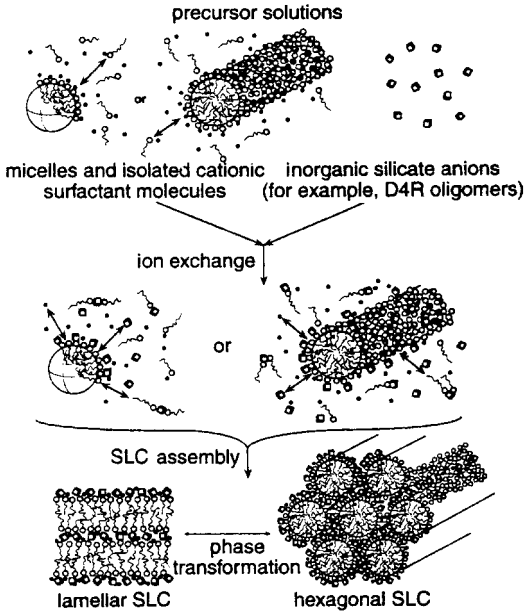

Scheme 7. Formation of a silicatropic liquid crystal phase.[18]

very similar to typical lyotropic systems, except that the surfactant concentrations were much lower and the silicate counterions were reactive.[20] Heating the SLC phase caused the silicates to condense irreversibly into MCM-41.

Firouzi and co-workers[18, 20] also demonstrated that in addition to the charge balance requirement (i.e., electrostatic interaction) there was preferential bonding of the ammonium

head group to multi-charged D4R (double four-ring, $[Si_8O_{20}]^{8-}$) silicate anions under the high pH conditions. The interaction was so strong that an alkyltrimethylammonium surfactant solution could force a silicate solution that did not contain D4R oligomers to re-equilibrate and form D4R species. It was suggested that this behavior came from the closely matched projected areas of a D4R anion and an ammonium head group (0.098 nm^2 vs. 0.094 nm^2) and the correct distribution of charges on the projected surfaces.

Fyfe and Fu[21] were able to prepare mesostructured silicates with D4R silicates. Combination of the D4R precursors with cetyltrimethylammonium chloride (CTAC) surfactants produced mesostructured precipitates. Control of the condensation of the silicates within the mesostructure by acidic vapor treatment led to the observation of cubic, lamellar, and hexagonal phases as intermediate transformation phases (see Section 2.1.3).

2.1.1.6. Silicate Rod Clusters

The previous theories have regarded the formation of MCM-41 as a series of events that occur homogeneously throughout an aqueous solution. Recent work has shown that MCM-41 might be formed heterogeneously. Regev[22] found evidence for MCM-41 intermediate structures in the form of clusters of rodlike micelles "wrapped" by a coating of silicate through low-temperature transmission electron microscopy (TEM) and small-angle X-ray scattering. The clusters of elongated micelles were found before precipitation occurred. As the reaction progressed, Regev proposed, the silicate species diffused to and deposited onto the individual surfaces of the micelles within the cluster; the clusters of elongated micelles eventually became clusters of silicate-covered micelles. Thus, the clusters of micelles served as nucleation sites for MCM-41 formation.

2.1.2. Generalized Liquid Crystal Templating Mechanism: Electrostatic Interaction

A generalized mechanism of formation based on the specific type of electrostatic interaction between a given inorganic precursor *I* and surfactant head group *S* was proposed by Huo and co-workers.[23] Based on the nomenclature, pathway 2 of the original LCT mechanism (Scheme 2), which involved anionic silicate species and cationic quaternary ammonium surfactant, could be categorized as the S^+I^- pathway. By extension, the other charge-interaction pathways are S^-I^+, $S^+X^-I^+$ (X^- is a counteranion), and $S^-M^+I^-$ (M^+ is a metal cation). This classification system is useful, especially when other types of inorganic–organic interactions are considered (Figure 1). The success of the cooperative templating model, referred to here as the generalized LCT mechanism (Scheme 8), was illustrated by the diverse compositions of organic–inorganic mesostructures found possible (see Section 2.3.1). As for silicate mesostructures, Huo and co-workers[23] found them possible through the $S^+X^-I^+$ pathway. By operating below the isoelectric point of silica (pH ≈ 2) under acidic conditions, the silicate species were cationic (I^+). The same ammonium surfactant S^+ could be used as a

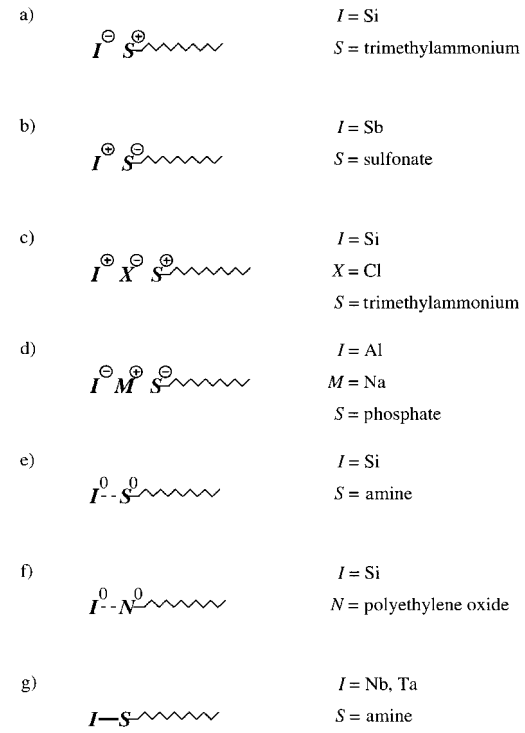

Figure 1. Schematic representation of the various types of inorganic–surfactant head group interactions: electrostatic: a) S^+I^-, b) S^-I^+, c) $S^+X^-I^+$, and d) $S^-M^+I^-$; hydrogen bonding: e) S^0I^0 and f) N^0I^0; and covalent bonding: g) *S–I*.

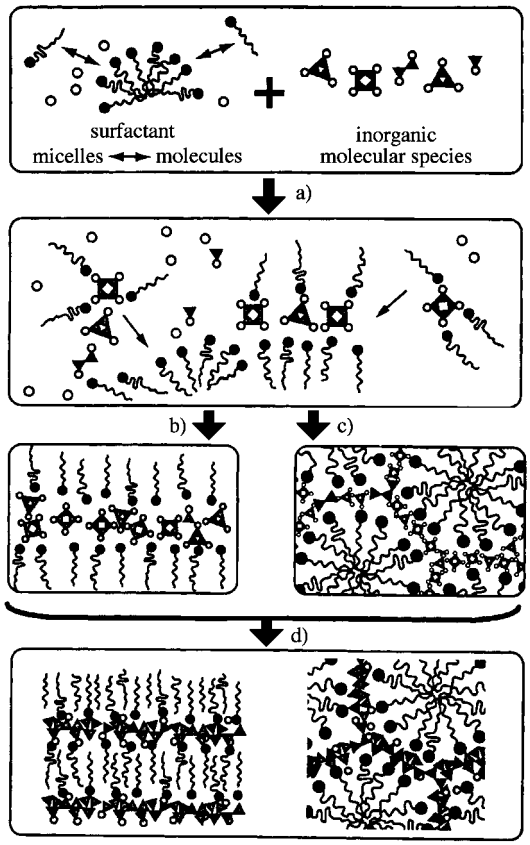

Scheme 8. Cooperative templating of the generalized LCT mechanism.[23b] a) Cooperative nucleation; b), c) liquid crystal formation with molecular inorganic compounds; d) inorganic polymerization and condensation.

templating agent but the halide counteranion X^- became involved through this pathway as it served to buffer the repulsion between the I^+ and S^+ by means of weak hydrogen-bonding forces. The resulting materials are known as "acid-prepared mesostructures" or APM materials.

2.1.3. Formation of Non-Hexagonal Mesophases

There are two synthesis routes for the derivation of silicate mesoporous molecular sieves of various mesophases: the basic route (S^+I^-) and the acidic route ($S^+X^-I^+$). Synthesized in basic medium, the M41S family is made up of three well-defined mesostructures: MCM-41, MCM-48, and MCM-50[24] (Table 2, Figure 2). MCM-41 has a hexagonally packed array

Table 2. Mesophases of silicate molecular sieves and governing synthesis parameters.

Name	Mesophase	Space group	Parameter
MCM-41[1, 24]	hexagonal[a]	*p6m*	[surfactant]/[Si] < 1
MCM-48[1, 24]	cubic	$Ia\bar{3}d$	[surfactant]/[Si] = 1 – 1.5
MCM-50[1, 25]	lamellar	*p2*	[surfactant]/[Si] = 1.2 – 2
SBA-1[23, 26]	cubic	$Pm\bar{3}n$	$g = 1/3$[b]
SBA-2[29]	hexagonal[c]	$P6_3/mmc$	$g < 1/3$[b]
SBA-3[26]	hexagonal[a]	*p6m*	$g = 1/2$[b]

[a] Two-dimensional array. [b] $g = V/a_0 l$. [c] Three-dimensional array.

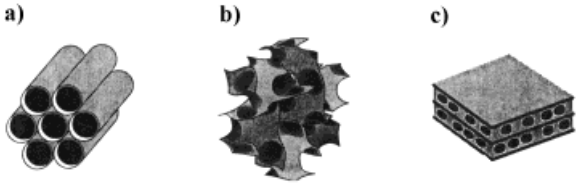

Figure 2. Illustrations of mesoporous M41S materials: a) MCM-41, b) MCM-48, and c) MCM-50.[3]

of noninterconnecting cylindrical pores. The structure of MCM-48 belongs to the cubic space group $Ia\bar{3}d$. The structure can be thought of as two intertwined networks of spherical cages separated by a continuous silicate framework. MCM-50 contains a lamellar structure in the uncalcined form; a mesoporous pillared layered material results when the surfactant is removed after post-treatment with TEOS.[25] Vartuli et al.[24] found that the surfactant:silicon molar ratio was the key synthesis parameter that determined the mesophase (Table 2). At ratios approaching 2:1, a "cubic octamer" structure was formed. The uncondensed material was composed of D4R silicate anions complexed with the surfactant; this molecular compound further supports the preferential binding of D4R silicates with ammonium surfactants.

Through the acidic route, APM materials termed SBA have been synthesized.[26] SBA-1 is cubic (space group $Pm\bar{3}n$, Figure 3),[23, 26] but not bicontinuous as in MCM-48 ($Ia\bar{3}d$); SBA-3 (space group *p6m*) is the APM mesostructural analogue of MCM-41. The acid-derived materials have thicker pore walls and a framework charge different from the base-derived mesoporous materials, due to the different precipitation conditions and charge balance requirements. For example, the overall framework charge of SBA-3 was slightly positive and so the surfactant and counterion species (S^+X^-) could be removed in ethanol under reflux. In contrast, the inorganic framework of MCM-41 was negatively charged and the surfactants could be washed out only with acidic alcohol under reflux.

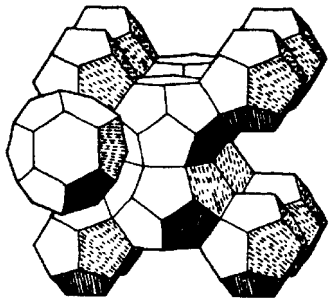

Figure 3. The $Pm\bar{3}n$ cubic phase, in which the polyhedra represent micelles.[27]

Another aspect of mesophase formation is the manner in which the surfactant tail groups pack in the material. Huo et al.[26] applied the concept of an effective surfactant packing parameter g ($g = V/a_0 l$) used for lyotropic LC phases to the silicate mesophases.[28] The packing parameter can be used to predict the phase of a given LC system as a first approximation; it is affected by the overall volume V of the surfactant, the effective head group area a_0, and the surfactant chain length l. Huo et al.[29] exploited this concept with the use of gemini surfactants (two ammonium surfactant molecules covalently linked through the head groups) to create SBA-2. The space group of SBA-2 is $P6_3/mmc$. Its structure consists of a hexagonal close-packed (hcp) array of spheres; the spheres can be thought of as spherical micelles. This structure is not found in the traditional LC systems. The preparation of MCM-48 ($Ia\bar{3}d$) was also demonstrated by adjustment of g with alcohol addition to the synthesis mixture[30] or with mixed cationic-anionic surfactants.[31]

2.1.4. Hydrogen-Bonding Interaction

Tanev and Pinnavaia[32] showed that mesoporous silica could be prepared by the hydrogen-bonding interaction of an alkylamine (S^0) head group and hydroxylated TEOS (I^0; Figure 1e). The materials lacked long-range ordering of pores and had higher amounts of interparticle mesoporosity, because the long-range effects of the electrostatic interaction that would normally control the packing of micellar rods were absent. This neutral templating synthesis route produced mesoporous silicates with thicker walls and higher thermal stability compared to the LCT-derived silicates.[33] The silicate framework in the resulting mesophase was neutrally charged, so the surfactants could be removed by solvent extraction. Tanev and Pinnavaia[34] further exploited the S^0I^0 route by the use of double-headed alkylamines (α,ω-dialkylamine) to create porous lamellar mesostructures.

Another hydrogen-bonding synthesis route used surfactants with a polyethylene oxide head group (Figure 1f).[35] Because the length of the head group and that of the tail group could be adjusted, pores as large as 58 Å could be synthesized without the use of swelling agents. The polyethylene oxide head group is nonionic (N^0), unlike the amine head group (S^0) which is uncharged and can be ionized. The nonionic route (N^0I^0) seemed to provide greater pore ordering than the neutral route (S^0I^0), but still lacked long-range hexagonal packing order. The pores were more "wormlike" than rodlike cylinders.

2.1.5. True Liquid Crystal Templating Mechanism

By operating in the liquid crystal phase region of a polyethylene oxide surfactant solution, Attard et al.[36] showed that monolithic mesoporous silicates could be prepared. Tetramethylorthosilicate (TMOS) was gelled in the LC solution with removal of the LC-destabilizing methanol, to produce a hexagonal mesophase; the $Ia\bar{3}d$ and layered phases were found possible also, depending on the chain length of the tail group. This synthesis approach could be considered a true LCT route, which supports the viability of pathway 1 of the originally proposed LCT mechanism for MCM-41 (Scheme 2).[1b] In this method of preparation, the organic–inorganic interaction was less important than the actual presence of a LC phase. Göltner and co-workers[37] showed that amphiphilic diblock copolymers (with a polyethylene oxide head group and a polystyrene tail group) could also be used as templates to create crack-free monoliths of mesoporous silica.

2.1.6. Formation of Other Mesophases

Mesoporous silicates with pore systems not as well-defined as those of the M41S and SBA materials could result when an additional salt is added to the synthesis mixture. The structures of these materials deviate from the ideal hexagonal pore packing of MCM-41, as detected through XRD and TEM. The long-range ordering of the materials is not definitive proof for "better" materials, however. McGrath et al.[38] showed that a "sponge" phase (L_3) of mesoporous silicates could be induced by the use of cetylpyridinium bromide surfactant, hexanol co-surfactant, sodium chloride, and water as precursors. After the addition of TMOS and aging, the solution gelled into a monolithic form. The L_3 phase exists in lyotropic surfactant solutions but has no long-range ordering (Figure 4). Because of the special characteristics of the L_3 phase (which can be thought of as a random, bicontinuous cubic phase), the pore volume of the material could be controlled simply with the amount of water in solution, and surfactant removal was not required for mesoporosity.

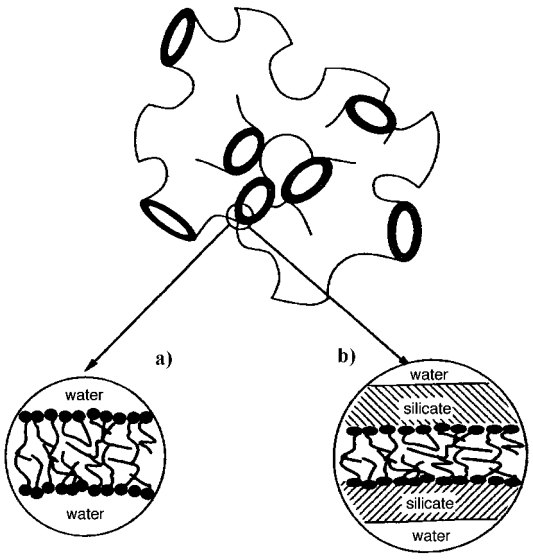

Figure 4. The silicate framework separates the water from the surfactants in the L_3 phase.[38]

In another approach, Ryoo and co-workers[39] added ethylenediaminetetraacetic acid (EDTA) to a high pH synthesis mixture, to create a hydrothermally stable mesoporous silicate with a highly branched network of pores similar to the L_3 surfactant phase (termed KIT-1). It was proposed that the EDTA polyacid salt caused the transformation of the hexagonal phase to the L_3-like mesophase.[39] For these disordered mesoporous materials, at least one strong XRD peak could still be detected in the low-angle region.

2.2. Doped Silicate Compositions

The interest in doping mesoporous silicates with metals lies primarily in the development of catalytically active materials. The incorporation of a metal is seemingly straightforward in light of the various mechanistic pathways, but the amount of dopant incorporation, the reproduction of the mesophase that is obtained in the pure silica system and the stability of the resulting mesoporous material cannot be predicted. In the original Mobil recipe, tetrahedrally coordinated aluminum atoms could be substituted isomorphously for silicon atoms in the MCM-41 framework as in the case for zeolites, but the degree of substitution depended on the aluminum precursor and method of preparation.[40, 45] The highest amount of aluminum that could be incorporated into the framework without formation of octahedrally coordinated aluminum (which does not belong to the framework) was reported to be about 9 mol %.[45] Fu et al.[46] reported the incorporation of up to 50 mol % Al into MCM-41 by means of special aluminosilicate ions ($[Al_4Si_4(OH)_8O_{12}]^{4-}$) with a similar cubelike structure as D4R silicates; however, the resulting materials showed little resemblance to MCM-41 and dealumination was reported. Ryoo et al.[40] showed that aluminum could be added to the synthesis mixture and be incorporated into MCM-41 even after the precipitation of the pure mesostructured silicate.

There are numerous reports that concern the doping of MCM-41 with a variety of metals (Table 3); the doped MCM-41 materials have been primarily used for catalytic applications (see Section 3.1). The amorphous silicate framework of MCM-41 could accept metal dopants other than aluminum but beyond a certain limit, the stability of the calcined material would become affected. Thus, the reported levels of doping for calcined MCM-41 were usually low, at most 1–2 mol %. The small amounts of metals that could be incorporated contrasted that of aluminum, probably due to the ease of substitution of the latter (which has a similar cation size and same coordination state as Si) into the silicate framework. Tuel and Gontier[52] showed that much higher loadings of tetrahedrally coordinated trivalent metal cations were possible through the "neutral" S^0I^0 route, rather than the electrostatic approach. The incorporation levels were apparently highly dependent on the synthesis route and sensitive to the pH of the synthesis mixture. Most doped MCM-41 materials were prepared under basic pH conditions (S^+I^-), whereas one set was prepared under acidic conditions ($S^+X^-I^+$)[56] with low incorporation levels (Table 3). In contrast, Wong et al. showed that MCM-41 type materials could be doped with very high

Table 3. Reports of dopant incorporation in silicate M41S materials.

Authors	Metal dopant	Si/dopant molar ratio	Synthesis route[a]
Beck et al.[1b]	Al	15	S^+I^-
Corma et al.[41]	Ti	56	S^+I^-
Reddy et al.[42]	V	60	S^+I^-
Tanev et al.[43]	Ti	100[b]	S^0I^0
Sayari et al.[44]	B	6.25[b]	S^+I^-
Luan et al.[45]	Al	10	S^+I^-
Fu et al.[46]	Al	≈1[b]	S^+I^-
Zhao, Goldfarb[47]	Mn	11	S^+I^-
Abdel-Fattah, Pinnavaia[48]	Sn	99	S^0I^0
Cheng et al.[49]	Ga	30	S^+I^-
Cheng, Klinowski[50]	Ga, Al	57, 57	S^+I^-
Koyano, Tatsumi[51]	Ti	80	S^+I^- (MCM-48)
Tuel, Gontier[52]	Al	6	S^0I^0
	Ga	31	S^0I^0
	Fe	55	S^0I^0
	B	17	S^0I^0
Tuel et al.[53]	Zr	17	S^0I^0
Ulagappan, Rao[54]	Cr	30[b]	S^+I^-
Zhang, Pinnavaia[55]	Ti	50[b]	S^+I^- (MCM-48)
	Cr	50[b]	S^+I^- (MCM-48)
	V	50[b]	S^+I^- (MCM-48)
Zhang et al.[56]	Ti	277, 76	$S^+X^-I^+$, S^0I^0
	V	434, 131	$S^+X^-I^+$, S^0I^0
	Cr	163, 70	$S^+X^-I^+$, S^0I^0
	Mn	3332, 118	$S^+X^-I^+$, S^0I^0
	Mo	95, 199	$S^+X^-I^+$, S^0I^0
Echchahed et al.[57]	Fe	40	S^+I^- (MCM-48)
He et al.[58]	Fe	52	S^0I^0
Jones et al.[59]	Zr	25	S^+I^-
Zhang, Ying[60]	Nb	10	S^+I^-
Wong et al.[61]	Zr	5	$S^+X^-I^+$

[a] MCM-41 structure, unless otherwise noted. [b] Molar ratio values of precursor mixture, not of calcined materials.

loadings of zirconium (≈17 mol%) through the $S^+X^-I^+$ route.[61] Zhang and Ying[60] found that up to 10 mol% Nb could be introduced into MCM-41 at high pH, which could then be used to anchor amine-substituted porphyrin molecules[151] (see Section 3.3).

2.3. Non-Silicate Compositions

2.3.1. Generalized Liquid Crystal Templating Mechanism—Early Efforts

The first foray into mesostructured materials of non-silicate compositions started with the generalized LCT mechanism of Huo and co-workers.[23] Mesostructured oxides were found possible for such metals as Sb, Fe, Zn, Pb, W, and Mo.[23, 62] However, most mesophases were layered and did not yield porous materials when the surfactants were removed. The few hexagonal phases derived underwent mesostructure collapse upon surfactant removal (either by solvent extraction or by calcination) probably due to the lack of complete condensation of the inorganic framework.

2.3.2. A Modified Sol–Gel Method

Our laboratory's initial research efforts led to the first reported synthesis of mesoporous transition metal oxides.[63] Mesoporous titanium oxide was obtained with titanium ethoxide as the metal precursor since, like other transition metal alkoxides, it is highly reactive in the presence of water. Left uncontrolled, titanium alkoxide would react and form an insoluble titanium oxide gel precipitate. Antonelli and Ying reasoned that if the hydrolysis and condensation rates were controlled with a chelating agent such as acetylacetone, titanium isopropoxide could form mesostructured titania in the presence of a surfactant solution.[63] This "modified sol–gel method" was successful in yielding the mesoporous materials, with the resulting product characterized with XRD, nitrogen adsorption and TEM. Surfactants with head groups that could interact with the titanium alkoxide led to titania mesostructures, and the phosphate surfactants were preferred for their thermal stability to 100 °C during aging. The resulting mesoporous materials were termed TMS1 (Tech molecular sieves). Though not quite as well-defined in its long-range hexagonal packing order as the MCM-41 silicates, Ti-TMS1 still possessed a narrow pore-size distribution and a high surface area of about 200 $m^2 g^{-1}$.

2.3.3. Ligand-Assisted Templating: Covalent Interactions

In a different synthesis approach, our laboratory has successfully derived mesoporous niobium oxide (Nb-TMS1) and tantalum oxide (Ta-TMS1) molecular sieves without the addition of chelating agents.[64–66] Instead of relying on charge interaction, the surfactants were pretreated with the metal alkoxides in the absence of water to form metal-ligated surfactants. The highest quality materials came from the use of amine surfactants, due to the strong affinity for nitrogen–metal bond formation between the surfactant head group and the niobium or tantalum alkoxide precursor. Upon addition to the alkoxide–surfactant solution, water acted as both a solvent and a reactant, to initiate surfactant self-assembly and alkoxide hydrolysis/condensation, respectively. In this ligand-assisted templating (LAT) approach, control of mesostructure phases was found possible by adjustment of the metal/surfactant ratio, and led to a family of mesoporous transition metal oxides analogous to the M41S family of aluminosilicates (Table 4).

Table 4. Mesophases of niobium oxide molecular sieves.

Name	Mesophase	Space group	Parameter
Nb-TMS1[64]	hexagonal[a]	$p6m$	[surfactant]/[Nb] < 1.25
Nb-TMS2[65]	hexagonal[b]	$P6_3/mmc$	[surfactant]/[Nb] = 1.5
Nb-TMS3[65]	cubic	$Pm\bar{3}n$	[surfactant]/[Nb] = 1[c]
Nb-TMS4[65]	lamellar	$p2$	[surfactant]/[Nb] = 2

[a] Two-dimensional array. [b] Three-dimensional array. [c] Prepared by vapor diffusion of water into synthesis mixture.

Our laboratory has also extended the LAT approach to synthesize mesoporous zirconium oxide, Zr-TMS.[67] Zr-TMS was derived with very high surface areas (as high as 560 $m^2 g^{-1}$) from zirconium *n*-propoxide and phosphate surfactant, though not with a well-defined mesoporous phase. Wong and Ying were able to show that surface areas, pore sizes, and pore volumes could be controlled in accordance with the chain lengths of templating alkylphosphate molecules (for carbon number $n = 4–16$).[68] As in the case of Ti-

TMS1, some phosphate head groups remained in the material after calcination, which could be exploited for acid catalysis (see Section 2.3.4.3). The interactions between zirconium alkoxide and various anionic and nonionic amphiphiles were explored;[68] the covalency of the interaction was deduced from NMR spectroscopic studies and the templating of Zr-TMS by short-chained amphiphilic molecules (see Section 2.4).

2.3.4. Other Compositions

Before we developed the modified sol–gel and LAT routes, we too began with the electrostatic approach in the attempt to prepare mesoporous transition metal oxides. Many of our attempts resulted in non-mesostructured amorphous oxides, in spite of the careful control of pH, aging temperature and period, and choice of metal-surfactant ratios and precursor salts. The generalized LCT mechanism could be used to explain the formation of mesostructures but, unfortunately it could not be used a priori to predict mesostructure formation, given a metal salt and a surfactant precursor.

For many mesostructured metal oxides prepared through an electrostatic approach via the generalized LCT pathway, the isolated mesostructured products were uncondensed transition metal salts and were unstable upon surfactant removal. Stein et al.[69] found this to be the case for tungstate ($[H_2W_{12}O_{40}]^{6-}$) and niobotungstate ($[Nb_xW_{6-x}O_{19}]^{(2+x)-}$, $x = 2-4$) Keggin ions, as did others, including Janauer et al.[70] (W, Mo, V) and Luca and co-workers[71] (V). Suib and co-workers found that mesoporous manganese oxides (termed MOMS) could be synthesized by adjustment of the oxidation state of the Mn-containing precursor.[72, 73] The pore structure of the resulting materials was less well-defined after calcination than that of mesoporous MCM-41 and TMS1. Interestingly, the framework walls were crystalline, and the material exhibited semiconducting properties.

2.3.4.1. Alumina

Bagshaw and Pinnavaia[74] used polyethylene oxide surfactants in the N^0I^0 nonionic route to template mesoporous alumina (termed MSU). The materials contained wormlike pore channels with surface areas of greater than 400 m^2g^{-1}. Vaudry et al.[75] synthesized mesoporous alumina with higher surface areas (710 m^2g^{-1}). Carboxylate surfactants were used as the templates but the average pore sizes could not be tailored by variation of surfactant chain lengths; an LCT mechanism (S^-I^+ pathway) was not apparent. Yada et al.[76] found that careful control of pH led to the preparation of mesoporous alumina (with the retention of the main XRD peak) by the S^-I^+ route.

2.3.4.2. Aluminophosphates and Vanadophosphates

There have been attempts to extend the surfactant templating synthesis technique to aluminophosphates. Lamellar aluminophosphates were prepared.[77, 78] Vesicular templating of the inorganic components was proposed to explain the formation of inorganic–organic bilayers organized as cylinders,[79] and particles patterned like exoskeletons of radiolarian organisms.[80]

Fluoride ions were used in the synthesis mixture as mineralizing agents by Feng et al.[81] to produce layered, hexagonal, and cubic phases of aluminophosphates. The mesostructures were unstable to calcination, however. Hexagonally packed mesoporous aluminophosphates were obtained by Zhao et al.[82] by the use of TMAOH to carefully control the pH. Chakraborty et al.[83] were able to substitute silicon atoms into mesostructured aluminophosphates, where upon calcination, mesoporous silicoaluminophosphates were obtained.

Vanadium phosphorus oxides (VPO) are useful as selective oxidation catalysts, and mesoporous VPO synthesis has been attempted by several groups.[84, 85] Mesostructured VPO materials were found possible, but accounts on surfactant removal either indicated collapse of the mesostructure[84] or provided insufficient information on the mesoporosity.[85]

2.3.4.3. Zirconia

Zirconium oxide is an interesting material catalytically and much effort has been devoted to the generation of a mesoporous form. Hudson and Knowles[86] used alkyltrimethylammonium halide to template zirconium hydroxide to produce pure zirconia with a high surface area. The templating effect was not seen in this synthesis, which resulted in broad pore-size distributions. A "scaffolding" mechanism was proposed in which the occluded surfactant basically acted as a filler to prevent the zirconia framework from collapsing during heat treatment. Reddy and Sayari[87] found that a zirconium oxide mesostructure could be produced with zirconium sulfate as the inorganic precursor in a $S^+X^-I^+$ synthesis route. The material was found to collapse upon calcination. Ciesla et al.[88] and Liu et al.[89] found that by ion-exchanging the occluded sulfate counteranions with phosphates, a microporous zirconium oxo-phosphate could be obtained. Ciesla et al.[88] also found that a microporous zirconium oxide stabilized with sulfates could be produced by use of a different precursor, for example a zirconium *n*-propoxide at low pH. A microporous oxide form of hafnium, a heavier congener of zirconium, was derived similarly.[90]

Pure zirconium oxide is a weakly acidic catalyst and is not useful for reactions that demand strong acidity. To increase acidic strength, modification of the pure zirconium oxide with anions or metal dopants is required. Mesoporous phosphated zirconium oxide, a moderately acidic material, was prepared through a one-pot synthesis with zirconium *n*-propoxide and alkylphosphates.[67, 68] The phosphate groups that remained after calcination enhanced the thermal stability (as in the case of microporous zirconium oxo-phosphates), and increased the acidic strength of the zirconia framework.

2.3.4.4. Metal Sulfides

A few examples of mesostructured metal sulfides have been reported. Stupp and co-workers[91] used a polyethylene oxide surfactant with a cadmium salt solution to obtain a hexagonal mesophase. The material was then exposed to hydrogen sulfide gas, which converted the cadmium salt to cadmium sulfide. Li et al.[92] derived a lamellar tin sulfide material with CTAB and tin chloride as precursors, and sodium sulfide as

the reducing agent. Surfactant removal was not possible from the CdS materials and probably not possible from the SnS_2 layered mesostructures.

2.3.4.5. Other Examples

Zhao and Goldfarb[93] reported the use of non-amphiphilic compounds to template oxides of magnesium and zinc into lamellar mesostructures. Disodium chromoglycate and flufenamic acid compounds self-assembled into a lyotropic chromonic phase and interacted with the metal precursor by means of S^+I^- electrostatic attraction. Self-assembly occurred with the flat aromatic molecules containing edgewise polar groups, which differed from the amphiphilic molecules normally used.

Attard et al.[94] templated platinum salts with the hexagonal phase of polyethylene oxide surfactants, and reduced the mesostructure (with hydrazine hydrate or less noble metals) to give mesoporous platinum metal with an average pore size of 30 Å. The mesoporous platinum did not possess a long-range hexagonal packing of the pores.

2.4. Control of Pore Sizes

There is no energetic limitation to the pore sizes possible in microporous and mesoporous silicates, as shown by Navrotsky et al.[95] It was found that MCM-41 and zeolites are only slightly less stable relative to the thermodynamically stable phase of silica, α-quartz, which suggests that the only limitation to the synthesis of porous structures is to find the appropriate kinetic pathways. In this respect, it may be easier to synthesize amorphous mesoporous MCM-41-like materials with smaller pores, rather than crystalline microporous zeolites with larger pores.

Sun and Ying[96] were able to control pore sizes between 5 Å and 20 Å by the use of short-chain alkylamines as supramolecular templates, allowing for systematic bridging of the mesoporous and microporous regimes. This work demonstrated for the first time that non-zeolitic microporous materials (TMS5) could be synthesized by supramolecular templating of small molecules, and could be composed of pure niobia. The amphiphilic molecules with a hydrocarbon chain length of n less than eight are normally too small to self-assemble in an aqueous solution and would be expected to behave as molecular templating agents (as in zeolite synthesis). However, the ligand-assisted templating technique provided a shielding effect by the inorganic components on the amphiphile head groups in such a way as to favor self-assembly versus solubilization of the templating agents. Thus, supramolecular templating was successfully extended to the systematic synthesis of microporous materials. This approach was further modified by Sun and Ying to produce microporous Nb-TMS6 with use of α,ω-dialkylamines.[97]

The use of short-chained amphiphiles has also led to the systematic derivation of micropores in zirconium oxide. Wong and Ying[68] used short-chained alkylphosphates to produce high surface area porous zirconium oxides modified by surface phosphate groups.

At the other end of the pore-size spectrum, hexagonally ordered mesoporous silicates with pores as large as 300 Å (SBA-15) were found possible by researchers at the University of California at Santa Barbara.[98] Nonionic triblock copolymers (polyethylene oxide/polypropylene oxide/polyethylene oxide) were used under acidic conditions (pH $\approx$ 1), and the templating was thought to occur through both electrostatic and hydrogen-bonding interactions.

3. Catalytic Applications

The unique physical properties of MCM-41 have made these materials highly desirable for catalytic applications. The extremely high specific surface areas are conducive to high catalytic activity. The large pore size (relative to that of microporous zeolites) allows for the fixation of large active complexes, reduces diffusional restriction of reactants, and enables reactions involving bulky molecules to take place. In spite of the one-dimensionality of its pore channels, MCM-41 has been the main focus of catalytic studies (rather than the other M41S mesoporous structures) because of its ease of preparation.

The first catalytic studies with mesoporous molecular sieves focused on metal-substituted MCM-41 materials in which the active species were incorporated into the silicate matrix. The reactions studied were mainly oxidation reactions and acid catalysis. The next stage of development of MCM-41-based catalysts involved the deposition of heteroatoms onto the surface of the mesoporous framework. Since then, a wide variety of applications have been established and the field is still expanding rapidly. More recently, research has been devoted to the fixation of catalytically active complexes onto the walls of the MCM-41 porous framework to combine the advantages of homogeneous catalysis with a heterogeneous catalyst support. Although extensive research efforts have been undertaken to explore the catalytic applications of modified MCM-41 materials, industrial use has so far been limited. Only a longer time frame will reveal if commercial applications of these systems will become feasible.

3.1. Metal-Substituted Mesoporous Molecular Sieves

3.1.1. Oxidation Reactions

Titanium silicate materials with MFI or MEL zeolite structure types (e.g. TS-1 or TS-2) have been investigated as olefin epoxidation catalysts.[99] Although zeolites such as TS-1 showed very high catalytic activity and selectivity, they could only be effective in the oxidation of small molecules. Larger molecules like cyclohexene were excluded from catalytic conversion due to the rather small pore size of the TS-1 material (5.3×5.5 Å). Consequently, a considerable amount of research was dedicated to the preparation of titanium-containing zeolites with large pores. The synthesis of a titanium-substituted β zeolite with BEA structure (7.6×6.4 Å) enabled the epoxidation of long-chain aliphatic olefins.

To catalyze bulkier substrates, it would be critical to develop molecular sieves with even larger pore sizes.

Soon after the Mobil announcement of the M41S materials, the synthesis of MCM-41 doped with titanium was reported simultaneously by two groups. Corma et al.[41] prepared Ti-MCM-41 with ionic surfactants under hydrothermal condition, while Tanev et al.[43] synthesized Ti-HMS with neutral primary amine surfactants in a room-temperature preparation. Both synthesis procedures led to the incorporation of catalytically active titanium sites into the mesoporous silicate matrix without significantly affecting the surface area and pore size, although the Ti-HMS material contained more interparticle mesoporosity.

Comparison study[41] of Ti-MCM-41 with Ti-β zeolite and Ti-ZSM-5 showed a higher catalytic activity for the former in the epoxidation of norbornene with *tert*-butyl hydroperoxide (TBHP) as oxidant. In the evaluation of the Ti-HMS catalyst,[43] the sterically more demanding substrate 2,6-di-*tert*-butylphenol (2,6-DTBP) was investigated. The aromatic compound was selectively oxidized to the corresponding quinone with H_2O_2. This study further illustrated that Ti-HMS gave a higher conversion rate than Ti-MCM-41 in the oxidation of 2,6-DTBP. The authors suggested that due to the exceptionally high textural mesoporosity of the catalyst, Ti-HMS has less diffusional limitation than Ti-MCM-41 and therefore superior catalytic activity for the oxidation of large organic substrates.

A further study on the selective oxidation of large organic molecules was undertaken by Reddy et al.[42] By the substitution of vanadium into the porous framework of MCM-41 through hydrothermal synthesis, they were able to prepare a highly active and selective catalyst for the partial oxidation of cyclododecane and 1-naphthol with H_2O_2 as oxidant. The same group also prepared a vanadium-containing mesoporous material, V-HMS, by a room-temperature synthesis route.[100] The resulting catalyst was evaluated for the oxidation of 2,6-DTBP with either H_2O_2 or TBHP. Compared to the Ti-HMS described earlier,[43] the V-HMS material showed higher catalytic activity for this reaction.

Gontier and Tuel[101] reported the successful application of transition metal (Ti and V) substituted mesoporous and microporous molecular sieves for the liquid-phase oxidation of aniline. Although conventional oxidation catalysts like TS-1 and ZSM-48 exhibited good activity, the reaction was limited by pore diffusion of products and reactants in the zeolites. By the use of ultra-large pore materials like the doped MCM-41, diffusion limitation was overcome and higher catalytic activities were observed.

Tuel et al.[53] showed that zirconium-containing mesoporous MCM-41 could be synthesized with hexadecylamine surfactant and zirconium isopropoxide at room temperature. The resulting material, designated Zr-MS, showed similar catalytic activity in the oxidation of aniline as the titanium-containing mesoporous material. However, it gave higher selectivity for alcohol in the epoxidation of norbonylene.

An interesting approach was undertaken by Vankelecom et al.[102] which involved the incorporation of Ti-MCM-41 catalyst into a partially polymerized polymethylsiloxane matrix. Catalytic results for the epoxidation of *cis*-cyclooctene with TBHP suggested an even higher conversion for the polymer-embedded Ti-MCM-41 than the free catalyst. This example illustrated that a combination of membrane technique and materials design could have a significant impact in the development of future catalyst technology. Although a variety of MCM-41 materials containing early transition metals has been prepared and investigated for oxidation catalysis, their activities were lower than the existing zeolite systems. In order to make a real impact in the area of oxidation catalysis, new systems must be as active as TS-1 materials while providing a mesoporous structure.

3.1.2. Acid-Catalyzed Reactions

The cracking activity and hydrothermal stability of aluminum-substituted MCM-41 materials were investigated by Corma et al.[103] It was shown that the activity of MCM-41 for a reaction catalyzed by strong acid sites, such as *n*-heptane cracking, was much lower than that of an ultra-stabilized Y (USY) zeolite, and similar to that of amorphous aluminosilicate. However, in the case of gasoil cracking, the greater accessibility of the large molecules to acid sites in MCM-41 relative to USY made the difference in activity much smaller between these two catalysts. In order to simulate fluidized catalytic cracking conditions, MCM-41 was steam treated. The resulting material showed a collapse of the porous structure, and the gasoil cracking activity was greatly diminished. The steam-treated MCM-41 was a much less active catalyst than steam-treated amorphous aluminosilicate.

An investigation of the hydrocracking abilities of aluminum-substituted MCM-41 for larger size molecules was carried out by Reddy and Song.[104, 105] Significant catalytic activity was obtained with 1,3,5-triisopropylbenzene (TIPB), to form mainly mono- and di-substituted isopropylbenzene. A conversion as high as 100% was achieved for the hydrocracking of TIPB by loading the MCM-41 aluminosilicate with platinum metal.

Extensive studies on cracking[106–112] and hydrocracking[113–119] over MCM-41 were undertaken by the Mobil researchers, but no commercial use has been established yet. An interesting approach was described by Degnan et al.[116] that combined modified MCM-41 materials with zeolites to give a mixed hydroprocessing catalyst. In this catalyst, MCM-41 provided an ultra-high surface area supporting the metal components (Ni/W or Pt) for hydrogenation reactions, while the zeolite provided the acidic functionality required for cracking. The resulting catalyst exhibited good activities in both hydrogenation and cracking, and could be used in fuel hydrocracking processes, especially where high conversion levels were desired.

An application of aluminum-containing MCM-41 was reported by Aguado et al.,[120] which showed the conversion of low-density polyethylene (LDPE) to hydrocarbon feedstock. Cracking of polyolefins typically involves solid acid catalysts, such as amorphous aluminosilicates and zeolites. Due to the bulky nature of the polymeric feedstock, catalytic activity has been mainly governed and limited by the catalyst pore size. Consequently, despite its lower aluminum content, aluminosilicate MCM-41 was found to be more active for LDPE cracking than amorphous aluminosilicate, due to its

greater mesoporosity. Although the reaction was hindered by its small pore size (≈5.5 Å), ZSM-5 showed the highest activity for the LDPE cracking since, in the earlier reaction stages, only acid sites located on or near the external surface were involved. The superior activity of ZSM-5 compared to MCM-41 was attributed to the higher acid strength of ZSM-5. However, the product distribution obtained with MCM-41 consisted of more liquid hydrocarbons in the range of gasoline and middle distillates with lower aromatic content relative to amorphous aluminosilicate and ZSM-5. This example showed quite nicely that even though MCM-41 materials could not compete in catalytic activity, they could produce new product distributions (i.e., favorable selectivity) that could be useful towards existing processes.

The application of aluminosilicate MCM-41 as a catalyst in the production of acetals was reported by Climent et al.,[121] and it represented a good example where the moderate acidity and the mesoporous structure of MCM-41 were well utilized. These acetal compounds are interesting for use in pharmaceuticals and as fragrances in perfumes and detergents. MCM-41 was shown to be an active and selective catalyst for the acetalization of aldehydes. For small aldehyde reactant molecules, zeolites were found to be more active than mesoporous MCM-41. However, when reactants larger than 7 Å were involved, geometrical constraints did not allow them to diffuse into the microporous framework of zeolites. The ultra-large pores of MCM-41 made this material more attractive for the acetalization of many fine chemicals.

Tetrahydropyranylation of alcohols and phenols represents a common synthetic tool to protect the hydroxyl functionality in peptide, nucleotide, carbohydrate and steroid chemistry. Kloetstra and van Bekkum[122] used aluminosilicate MCM-41 as a mild and efficient acid catalyst for the tetrahydropyranylation of primary, secondary, and tertiary alcohols and phenols. It was also shown that aluminosilicate MCM-41 provided excellent catalytic activity and selectivity with respect to bulky substrates like cholesterol, superior to the current commercial heterogeneous aluminosilicate catalysts.

The application of aluminosilicate MCM-41 as acid catalyst for Friedel–Crafts alkylation was reported by Armengol et al.[123] In this study, the bulky substrate 2,4-di-*tert*-butylphenol (2,4-DTBP, **1**) was alkylated with cinnamyl alcohol, to give a mixture of **3** and **4** together with minor amounts of **5** (Scheme 9). The formation of dihydrobenzopyran **3** was attributed to an intramolecular ring closure of the primary cinnamylphenol **2** that arose from the Friedel–Crafts alkylation of phenol **1**. The formation of **4** and **5** was suggested to be based on acid-catalyzed dealkylation, which has been frequently observed for *tert*-butyl-substituted aromatic compounds. MCM-41 was shown to give higher yields of **3** than conventional catalysis with sulfuric acid or amorphous aluminosilicate. No reaction occurred over acid faujasites (HY) and only very little activity was noted for steam-treated HY zeolite.

Alkylation reactions of naphthalene, paraffin, and benzene with short- and long-chain olefins were also examined over MCM-41.[124–127] MCM-41 was found to be less reactive than ZSM-5 in the synthesis of ethylbenzene, but it yielded more polyalkylated products than the latter.

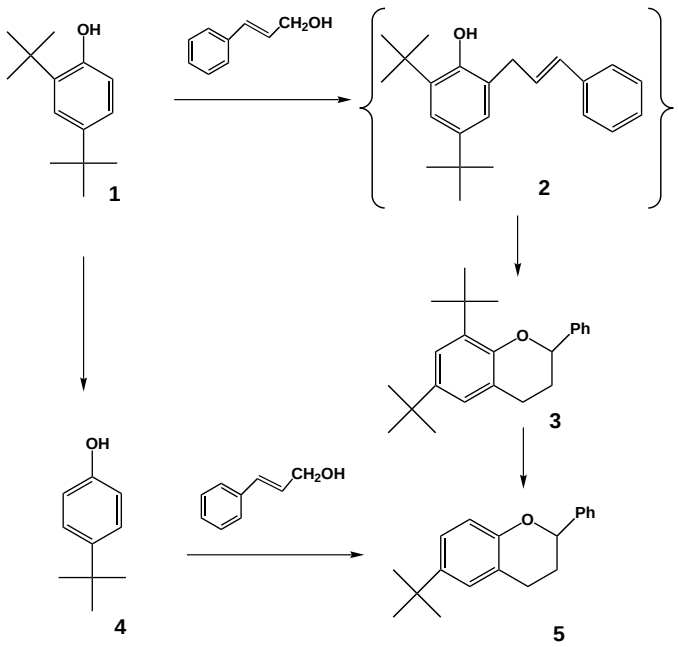

Scheme 9. Alkylation of 2,4-DTBP with cinnamyl alcohol over aluminosilicate MCM-41.

By introducing titanium into the framework of aluminosilicate MCM-41, a bifunctional catalyst was prepared by Corma et al.[128] for the conversion of linalool into cyclic furan and pyran hydroxyl ethers (Scheme 10). The authors

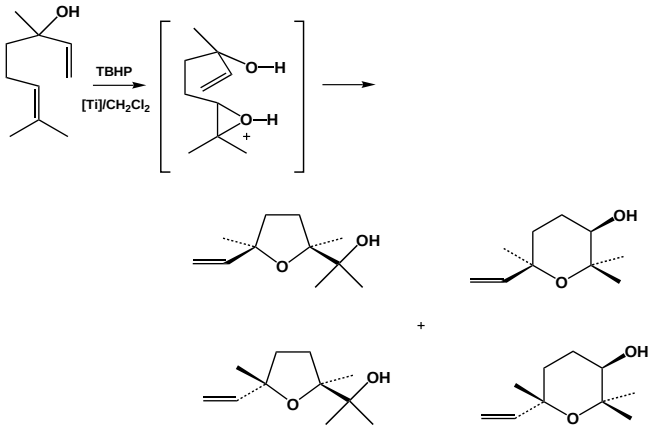

Scheme 10. Conversion of linalool into cyclic furan and pyran hydroxyl ethers with Ti-MCM-41 ([Ti]).

postulated that epoxidation took place over the titanium sites, and acid-catalyzed intramolecular ring opening of the epoxide then occurred by the 3-hydroxyl group. The conversion for this reaction was as high as 80 % with the Ti-MCM-41 material. In comparison, titanium-modified zeolite β gave somewhat lower conversion. Although Ti-β zeolite usually exhibited higher activity than Ti-MCM-41 in epoxidation reactions, Ti-MCM-41 provided greater activity in this case, possibly due to increased diffusion of reagents through its larger pores.

Deviating from the typical aluminosilicate compositions, phosphated mesoporous zirconium oxide (Zr-TMS) was developed for mild acid catalysis.[67, 68] The Zr-TMS material

was found to be active for the gas-phase double-bond isomerization of 1-butene at temperatures of 100–350 °C. The material should also be useful for other types of reactions that require moderate acidity, and was seen as an improvement over crystalline layered zirconium phosphates for acid catalytic applications.

3.1.3. Hydroxylation Reactions

The catalytic hydroxylation of benzene to phenol over a variety of transition metal substituted mesoporous molecular sieves was reported by Zhang et al.[56] Ti-, V-, Cr-, Mo-, and Mn-substituted MCM-41 and HMS silicates (with typical transition metal contents of 0.2–1.5 wt %) were prepared by electrostatic and neutral templating pathways, and examined for the peroxide hydroxylation of benzene. All materials were catalytically active, and in particular the Ti-HMS material gave ≈100 % selectivity at low conversion. In a further study by the same group,[55] transition metal (Ti, V, Cr) substituted cubic-phased MCM-48 mesoporous silicates were prepared by hydrothermal synthesis, and successfully applied for the selective peroxide oxidation of styrene and methyl methacrylate to benzaldehyde and methyl pyruvate, respectively.

3.1.4. Polymerization Reactions

In a study by Abdel-Fattah and Pinnavaia,[48] tin-substituted mesoporous silicate was prepared by neutral amine surfactant assembly of silicon and tin(IV) alkoxides at ambient temperature. The resulting material was successfully applied to lactide ring-opening polymerization. Sn-HMS yielded higher conversion than tin-doped silica and pure tin oxide. Compared to homogeneous catalysts, Sn-HMS improved the average molecular weight and polydispersity of polymers produced, possibly by imposing steric constraints on the propagating polymer chain with its ordered pore structure, and by minimizing "back-biting" and intermolecular transesterification reactions.

3.2. Metal-Deposited Mesoporous Silicates

One of the earliest catalytic applications of MCM-41 involved supported NiMo in gasoil hydrocracking.[103] The molybdenum and nickel components were introduced by the incipient wetness impregnation technique, followed by calcination. Despite a loading of 12 wt % MoO_3 and 3 wt % NiO, the surface area of the MCM-41 support was only slightly reduced. The NiMo-MCM-41 catalyst showed a higher hydrodesulfurization and hydrodenitrogenation activity than NiMo loaded on USY or amorphous aluminosilicate. The better performance of NiMo-MCM-41 was attributed to the mesoporous structure and the high surface area that provided access to bulky molecules and a high dispersion of active metal components.

The application of modified MCM-41 material in the reduction of nitrogen oxides (NO_x) from emission gases has been reported by Beck et al.[129] The molecular sieves were used as a framework for the deposition of vanadium and titanium oxides. It was found that the modified MCM-41 material exhibited higher activity for NO_x reduction by ammonia than vanadium oxide and titanium oxide loaded amorphous silica gel.

Another interesting application of modified MCM-41 material was reported by Kresge et al.[130] for the demetalation of hydrocarbon feedstock. MCM-41 was loaded with MoO_3 and NiO by impregnation. This catalyst showed a high efficiency for the removal of iron and nickel, and was also active for arsenic removal and desulfurization.

For the oligomerization of α-olefins, Pelrine and co-workers[131, 132] reported the use of chromium-modified MCM-41 material. The metal component was introduced through impregnation, followed by calcination to give chromia-loaded MCM-41. Prior to polymerization experiments, the material was activated by carbon monoxide to reduce the chromium to a lower valence state. Oligomerization of 1-decene over this catalyst produced a wide variety of lubricants with higher viscosity values than those obtained with chromia on silica.

The use of nickel-impregnated MCM-41 aluminosilicate for oligomerization of olefins was reported by Bhore et al.[133] Compared to zeolites with medium pore sizes, the impregnated MCM-41 material showed higher activity and greater selectivity for the formation of trimers and tetramers of propylene. Furthermore, they offered control over the degree of branching through variation of the reaction conditions.

The isomerization of *n*-hexane with platinum-modified MCM-41 aluminosilicate was reported by Del Rossi et al.[134] The platinum precursor $[Pt(NH_3)_4Cl_2]$ was introduced by ion exchange, and the material was then calcined. Although platinum on amorphous SiO_2-Al_2O_3 showed a slightly higher conversion of *n*-hexane than Pt-MCM-41, the selectivity for isohexane was significantly higher over Pt-MCM-41 with its uniform pore structure.

Borghard et al. investigated the hydrogenation of benzene to cyclohexane, and showed that Pd-impregnated MCM-41 has higher activity than palladium supported on other materials.[135] The enhanced reactivity was attributed to the higher surface area and pore volume of the MCM-41 support.

An alternative approach in acid catalysis was described by Kresge et al.[136] Instead of modification of the silicate framework of MCM-41 with trivalent cations (e.g. Al^{3+}) to generate Brønsted acid sites, they deposited heteropolymetallic acids inside the porous framework. Although heteropolymetallic acids have very strong acid sites, their surface areas are rather small. By utilizing supports with high surface areas, acid site dispersion was achieved. The catalyst was prepared by loading the mesoporous material with phosphotungstic acid ($H_3PW_{12}O_{40}$) with the incipient wetness method, and was investigated for four different paraffin substrates. In *n*-butane conversion, isobutane was obtained with a selectivity exceeding 80 %, which was substantially higher than that achieved over ZSM-5. For the conversion of *n*-hexane, the heteropolymetallic acid loaded MCM-41 exhibited higher activity (with comparable selectivity), compared to Pt-MCM-41. The excellent activity was attributed to the high dispersion of the heteropolymetallic acid on MCM-41.

Aluminosilicate MCM-41 materials cation-exchanged with sodium and cesium have been successfully used for the base-

catalyzed Knoevenagel condensation.[137] The reaction of benzaldehyde and ethyl cyanoacetate in aqueous solution in the presence of Na-MCM-41 (Scheme 11) led to a conversion

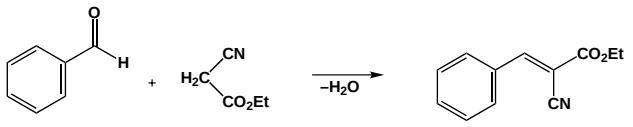

Scheme 11. Base-catalyzed Knoevenagel condensation over MCM-41 cation-exchanged with sodium and cesium.

of about 90 % within three hours with almost 100 % selectivity. In contrast, the same reaction in boiling ethanol led to the acetalization of benzaldehyde due to the presence of residual acid sites. Furthermore, both H-MCM-41 and Na-MCM-41 catalyzed the condensation of benzaldehyde with acetophenone to yield chalcone. They were also successfully employed for aldol condensations with bulky ketones. In addition, if an α-hydroxyl group was present on the benzophenone, an intramolecular Michael addition giving flavanone would follow the aldol condensation (Scheme 12).

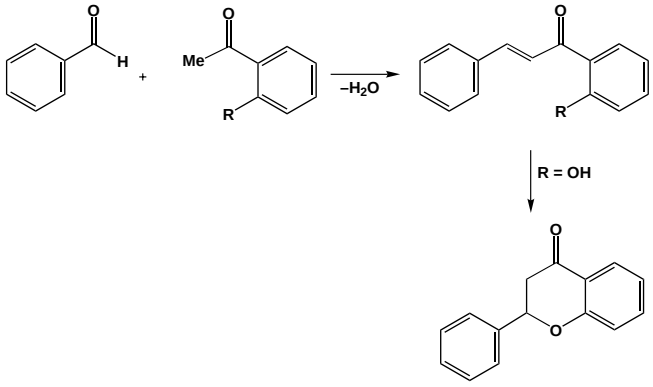

Scheme 12. Aldol condensation between benzaldehyde and acetophenone, followed by a Michael addition to give flavone, over H-MCM-41 and Na-MCM-41.

One of the first examples of the deposition of active metal oxide sites on MCM-41 through the fixation of organometallic complexes onto the inside walls of MCM-41 was reported by Maschmeyer et al.[138] Treatment of the porous MCM-41 material with a solution of $[(C_5H_5)_2TiCl_2]$ in the presence of NEt_3 anchored the titanocene complex through oxygen atoms onto the pore surface. Calcination under a stream of oxygen removed the cyclopentadienyl ligand and generated an active epoxidation catalyst. The resulting system showed good activity, and was particularly useful in the conversion of bulky substrates, which could have access to the active centers inside the ultra-large pores. With the same approach, vanadium-grafted[139] and manganese-grafted[140] MCM-41 materials were derived and their applications as oxidation catalysts were demonstrated.

A major drawback of the "wet" impregnation method is the undesired cluster growth during the deposition of the active species. In order to overcome this problem and to ensure a high dispersion of active species, a new methodology, termed vapor grafting, was developed by Ying and Mehnert.[141] By use of volatile organometallic precursors, it was possible to deposit active species in a highly dispersed and uniform fashion throughout the entire porous system of MCM-41 (Figure 5). The resulting variety of metal and metal oxide

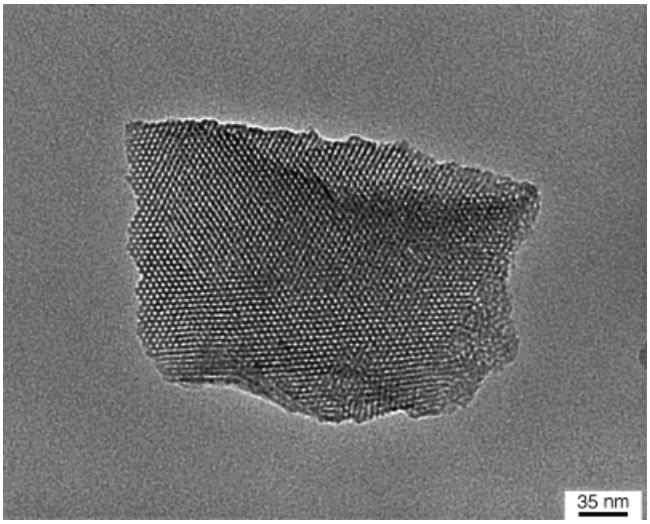

Figure 5. TEM image of the palladium-grafted mesoporous silicate material Pd-TMS11.[142]

grafted mesoporous materials (termed TMS11) presented an attractive combination of ultra-high catalyst dispersion and tunable pore sizes (15 – 100 Å). The Pd-TMS11 material[142, 143] was conveniently prepared by vacuum sublimation of $[CpPd(\eta^3\text{-}C_3H_5)]$ through the hexagonally packed MCM-41 mesopores, followed by reduction under hydrogen. Investigation of Pd-TMS11 for carbon – carbon coupling reactions (Heck reaction, Scheme 13) showed that its catalytic activity was superior to that of other heterogeneous Heck catalysts

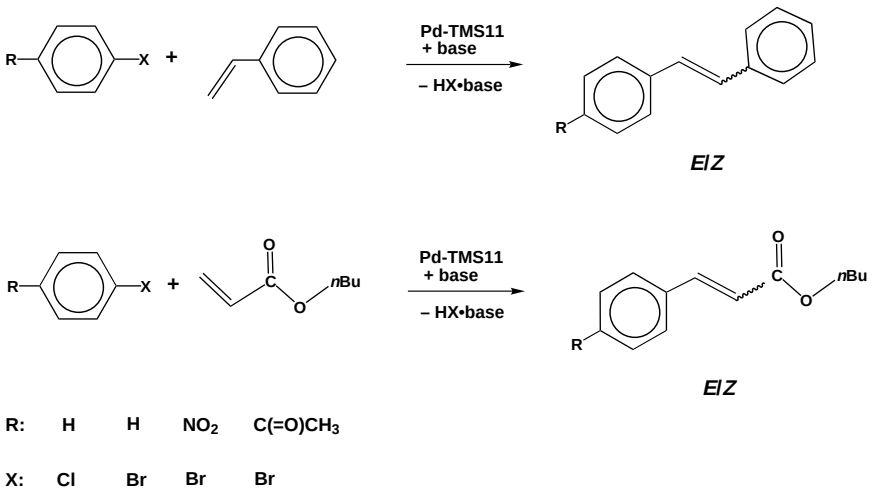

Scheme 13. Carbon – carbon coupling reactions catalyzed by mesoporous Pd-TMS11 material.

and even surpassed that of many homogeneous catalysts. This heterogeneous Heck catalyst demonstrated how bulky substrates could be effectively and selectively coupled to an even larger molecule inside the mesoporous framework. The highly dispersed Pd-grafted catalyst provided a less expensive and more thermally robust alternative to homogeneous Pd complexes.

3.3. Organometallic Complexes Anchored to Mesoporous Silicates

An early example for the anchoring of an organometallic complex onto the porous walls of aluminosilicate MCM-41 was reported by Liu et al.[144] They treated ion-exchanged MCM-41 with phenanthrolineiron(II) chloride and were able to immobilize the complex. The resulting material was investigated for the oxidation of phenol with H_2O_2 as the oxidant. A higher activity was obtained with the immobilized iron complex than for the free iron complex. However, a significant amount (9.5%) of leaching was noted in the former, which could be overcome when the transition metal complexes were anchored onto the walls of MCM-41 with an organic linker.

Sutra and Brunel[145] treated MCM-41 material with $(MeO)_3Si(CH_2)_3Cl$, which generated surface-bound 3-chloropropylsilane moieties that could be allowed to react with bis-3-(3,5-di-*tert*-butylsalicylidenaminopropyl)amine, to yield surface-bound Schiff base ligands (Scheme 14). The metal was

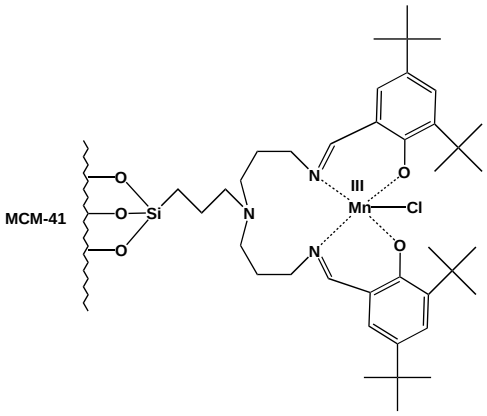

Scheme 14. Surface-fixated Schiff base ligand with coordinated manganese for epoxidation reactions.

then introduced by means of a solution of $[Mn^{II}(acac)_2]$ (acac = acetylacetone) in methanol. Air oxidation of the solution gave the final Mn^{III} complex. The immobilization of such epoxidation catalysts offered the advantage of easy separation and the potential of increased selectivity with the well-defined pore structure of the support material.

Surface-immobilized manganese–triazacyclononane complexes have also been developed for epoxidation catalysis.[146] By anchoring 1,4,7-triazacyclononane on glycidylated MCM-41, followed by the introduction of the manganese metal, a catalyst with remarkable epoxidation activity and high selectivity for styrene and cyclohexene was achieved.

Cobalt(II) complexes have been immobilized onto the inside walls of ethylenediamine-grafted mesoporous materials.[147] For the functionalization of the support, the surface-bound silanol groups were allowed to react with alkoxysilyl compounds that possessed donor amine groups to produce chelating ligands that were then used in the complexation of metal ions such as Co^{II}. The ability of the cobalt–amine complexes to form reversible dioxygen adducts was also demonstrated and might be useful to some biological reactions.

Although numerous efforts have focused on the fixation of metalloporphyrins, as in the elegant work of Herron and coworkers[148, 149] who reported the entrapment of phthalocyanine within large pore zeolites, turnover frequency and selectivity were rather poor. More recently, the encapsulation of ruthenium porphyrins in modified MCM-41 was reported by Liu et al.[150] In this work, the surface of MCM-41 was treated with 3-aminopropyltriethoxylsilane to provide a two-electron donor anchor (NH_2 group) to which the ruthenium porphyrin was attached (Scheme 15). The catalyst derived was

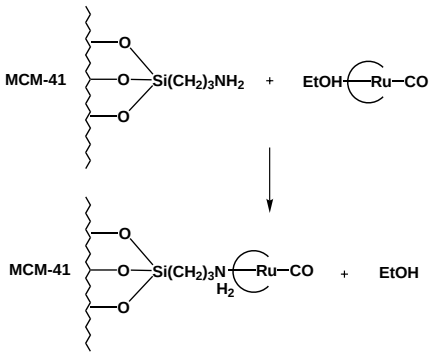

Scheme 15. Surface-immobilized ruthenium porphyrin complex on MCM-41.

investigated for the oxidation of olefins, giving turnover numbers that were 20–40 times higher than that for the free porphyrin. Also of interest was the observation that in the oxidation of *cis*-stilbene with the modified MCM-41 material, the major product was *trans*-stilbene oxide. In contrast, oxidation of *cis*-stilbene catalyzed by free ruthenium porphyrin gave a 1:1 mixture of *cis*- and *trans*-stilbene oxides. The high selectivity to *trans*-stilbene oxide was attributed to the steric constraint imposed by the straight channels of the MCM-41 support. This example demonstrated nicely the potential of mesoporous materials in size- and shape-selective catalysis.

An alternative approach in the anchoring of metalloporphyrin onto the inside walls of mesoporous MCM-41 has been developed by Zhang et al.[151] with amine-substituted porphyrin systems. The active complex was attached by means of a covalent interaction between the amine terminal groups of the complex and the niobium dopants in the support matrix. Such ligation ensured that the active sites would not undergo self-oxidation. Excellent cyclohexane hydroxylation and cyclohexene epoxidation activities have been obtained with this catalyst system, and the material could be recycled for

repeated use without loss of activity or leaching of porphyrin complexes.

An interesting approach was taken by O'Brien et al.,[152] whereby the MCM-41 material was modified with ferrocenyl end groups attached to the silicate surface. By means of the ring-opening reaction of the strained metallocenophane [Fe{(η-C_5H_4)$_2$$SiMe_2$}], it was possible to anchor ferrocenyl units inside the pore channels of MCM-41. This fixation reaction demonstrated the potential of these mesoporous molecular sieves as a matrix for the encapsulation of defined organometallic complexes.

A further example for the attachment of a well-defined cobalt oxide species was reported by Maschmeyer et al.[153] They investigated the selective oxidation of cyclohexane to cyclohexanone using a cobalt complex that was bound either directly to a hydroxyl group of the MCM-41 surface or to a surface-anchored spacer compound which contained a carboxylic acid group. The evaluation of the catalysts showed that the directly anchored complex had a lower conversion than the complex that was attached through the spacer. Although this catalyst system exhibited only mediocre activity (12% conversion after 24 hours), no leaching of the cobalt cluster was apparent. The high stability against leaching was attributed to the anchoring of the cluster to the functionalized MCM-41 surface.

Two independent groups have reported the preparation of MCM-41 grafted with methylalumoxane (MAO) for use as support for catalysts in Ziegler–Natta polymerization.[154, 155] The immobilization of homogeneous metallocene catalysts onto support materials has been of great interest since fixation of the polymerization catalysts to a surface might enable polymers to be replicated with higher density and larger particle size than those produced by unsupported homogeneous catalysts. In the catalyst preparation by Tudor and O'Hare,[155] dehydrated MCM-41 material was first treated with an excess of MAO, and then with the chiral polymerization catalyst *rac*-ethenebis(indenyl)zirconium dichloride. It was found that the polypropylene produced by the metallocene-grafted MCM-41 was fourfold higher in number-averaged molecular weight and has higher isotacticity and melting point than that produced by the homogeneous catalyst.

An alternative approach in the fixation of polymerization catalysts has been developed by immobilizing zirconocene complexes[156] that have modified cyclopentadienyl ligands. These zirconocene complexes could be conveniently anchored onto the walls of MCM-41 materials through their siloxy groups (Scheme 16). This catalyst system showed remarkable reactivity for ethylene polymerization; however, low activity was observed for propylene polymerization.

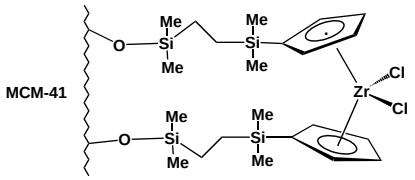

Scheme 16. Zirconocene complex anchored on the MCM-41 surface.

4. Other Applications

4.1. Thin Films and Membranes

In addition to catalytic applications, the well-defined mesoporous M41S family of materials also offer interesting potential for use in membrane separation, adsorption, and electronic/optical applications. For membrane applications, it is important to be able to process mesoporous structures in the form of defect-free, oriented thin films. Synthesis of ordered films of hexagonally packed mesoporous silica was first reported by Yang et al., who used an acidic aqueous mixture of cationic CTAC surfactant and TEOS.[157] Thin films (0.2–1.0 μm) could be grown from the bottom side of a cleaved mica substrate held horizontally in the synthesis vessel. Mesoporosity of the thin films became accessible upon calcination, and TEM revealed that the pore channels ran predominantly parallel to the mica surface. The formation of the oriented mesoporous silica films was thought to begin with nucleation which involved silica-surfactant-mica interfacial interactions that facilitated the assembly of silica-surfactant micellar seeds on the mica. A later study by Yang et al.[158] showed that ordered mesoporous films could be grown without a solid substrate by surfactant templating at the interface between air and water. These continuous films were believed to be formed through a dual-templating role of the surfactants. The authors suggested that the surfactant overstructure at the air–water interface and the micellar aggregates in solution interacted collectively with the soluble silicate building blocks to polymerize mesostructured silicates as free-standing films.

Aksay et al.[159] showed that continuous mesostructured silica films could be grown on many substrates, with the corresponding structure determined by the specifics of the substrate–surfactant interaction. For example, not only the hydrophilic surface of mica but hydrophobic surfaces such as graphite could be used as binding sites for the silica–surfactant micellar precursor species to orient a hexagonal phase of mesostructured silica in the form of a continuous thin film. This study presented XRD results that illustrated epitaxial alignment of the adsorbed surfactant layer with crystalline mica and graphite substrates. The presence of significant strain in the mesostructured silica overlayer was verified, and as the films grew thicker, accumulated strain was released, which resulted in the growth of hierarchical structures from the ordered film.

By slow evaporation of a sol mixture containing TMOS, two equivalents of water, CTAC, and a mineral acid, Ogawa[160] prepared a self-supporting transparent film of hexagonal-phase mesostructured silica. Transparency was retained after calcination, but the author did not discuss the orientation of the hexagonally packed pores or the retention of crack-free films.

For many potential applications, such as membranes for biomolecular separations and sensors for large molecules, it would be particularly useful to have the axis of the pore channel oriented vertically (instead of parallel) with respect to the solid substrate or liquid surface. The use of external forces to influence the ordering of pores in mesoporous films

has been examined recently. Hillhouse et al.[161] have prepared hexagonally packed mesoporous silica layers on glass substrates in a continuous flow cell, and showed that an external flow field could induce a preferred orientation for film formation. Tolbert et al.[162] demonstrated that the application of a strong magnetic field (11.7 T) could force the long-range orientational ordering of the pores in MCM-41 during the co-assembly process.

Lu et al.[163] found that oriented mesostructured films could be obtained by dip-coating substrates with dilute precursor sols. Slow evaporation of the solvent in the entrained solution drove the surfactant concentration past the CMC, and the co-assembly of the silicate and surfactant into a well-defined mesostructure. Depending on the initial surfactant concentration, mesostructured films with hexagonal, cubic, and layered phases could be prepared. With calcination, supported mesoporous films of the two-dimensional hexagonal phase (with pore channels parallel to the air–solid interface) and a mixed cubic and three-dimensional hexagonal phase were obtained. The mixed-phase film contained three-dimensional pore channels accessible from the air–solid interface. Lu and co-workers further reported the in situ study of the lamellar → cubic → hexagonal mesostructure phase transformations. Whereas Lu et al.[163] used CTAB as the templating surfactant, Tolbert et al.[164] employed a gemini surfactant to prepare a mesoporous silicate film with the three-dimensional $P6_3/mmc$ mesophase structure.[26, 29]

4.2. Hollow Tubules and Other Bulk Morphologies

The processing of mesoporous materials into designed bulk morphologies is not limited to thin films. Lin and Mou[165] have found that hollow tubules of 0.3–3 μm in diameter could be produced by careful control of the surfactant-water content and the rate of silica condensation at high pH values. The wall of these tubules consisted of coaxial cylindrical MCM-41 mesopores. It was proposed that solvent-separated multilayers of periodic hexagonal MCM-41 silicates could be formed and further "bent" into hollow microtubules with the nanochannels constituting the walls of these tubules. The hierarchical order of this "tubules-within-a-tubule" organization is similar in nature to that of the frustules of marine diatoms, and may find applications in catalysis, separation technologies, and optoelectronics.

While MCM-41 synthesis typically resulted in precipitated powders, Huo et al.[166] demonstrated that mesoporous silica could be produced in the form of marblelike spheres of about 1 mm in diameter. The authors prepared a basic CTAB solution and slowly added tetrabutylorthosilicate (TBOS) while stirring; the stirring speed controlled the size of the spheres. The surfactant was removed by calcination to yield smaller-diameter spheres of mesoporous silica. The authors suggested that the formation of the spheres was based on an emulsion synthesis, wherein the mixture of butanol (from hydrolyzed TBOS) was stabilized by the CTAB surfactant. The use of microemulsions was shown earlier in the formation of mesoporous silicate spherical shells by Schacht et al.[167]

MCM-41 powders typically have little form, because of the uncontrolled precipitation of these materials. Exceptions have illustrated the hexagonal habit of MCM-41[1b] and Nb-TMS1.[65] Interesting particle morphologies of APM materials (mesoporous silicates prepared under acidic conditions) were demonstrated by Ozin and co-workers.[168] The materials were synthesized under very low pH conditions and high dilution of TEOS and surfactant. These extreme synthesis conditions prevented uncontrolled precipitation of the mesostructured silicates, which allowed for high-curvature particles to nucleate and grow.

4.3. Other Templated Mesostructures and Hierarchical Structures

In the synthesis of MCM-41, ordered arrangements of mesoporous channels were produced in silica-based materials upon surfactant removal. The resulting pore sizes were governed by the diameter of the templating micelles, and have been limited to ≤ 30 nm. Recently, Davis et al.[169] showed that a bacterial superstructure, which consisted of a thread of coaligned multicellular filaments of *Bacillus subtilis*, could be used to extend the length scale of inorganic materials patterning. Ordered macroporous fibers of either amorphous silica or MCM-41 mesostructured silica were obtained by template-directed mineralization of the interfilament spaces, followed by removal of organic material by calcination. The resulting inorganic structures consisted of a macroporous framework of 0.5 μm wide channels with curved walls of either amorphous or mesoporous silica, 50–200 nm in thickness. This work illustrated how supramolecular and supercellular templates might be combined for the fabrication of inorganic materials with hierarchical structures.

The concept of supramolecular templating was also extended to porous silicates with a layered structure.[34, 170] Galarneau et al.[170] showed that mesoporosity could be introduced into layered silicate clays by a gallery-template synthesis, which extended the range of pore sizes possible in pillared layered silicates (from spacings of <10 Å to 14–22 Å). A cationic ammonium surfactant was used to swell a silicate clay before shorter chained alkylamines and TEOS were added; the organic components were later removed by calcination to yield porous clay heterostructures (PCH). The templating organics not only swelled the layers for the TEOS to pillar, but also controlled the spacing between the pillars within the galleries, an advantage not offered by traditional pillaring methods. Although the resulting materials did not resemble the typical M41S-type mesoporous materials, this approach could be applied to other classes of layered materials, such as zirconium phosphates.

4.4. Adsorbents

Beside catalysis and membrane separation, a major potential application of mesoporous materials lies in adsorbents. The huge pore volume and the compositional flexibility of MCM-41 type materials can be widely exploited for selective

adsorption of gases and liquids, and binding of metals. For example, Ioneva et al.[171] have shown that adsorptive storage of methane in silicate-based MCM-41 was possible at 25 °C up to 6.9 MPa. An increase in methane storage could be attained with increasing surface area per unit volume of adsorbent. MCM-41 allowed for a 75% improvement in the methane storage density over that of the compressed gas at 3.45 MPa. It also has higher total storage capacities for argon, nitrogen and light hydrocarbon vapors than typical microporous sorbents. In some applications, such as methane adsorption, pores smaller than 20 Å might be desirable for optimization of the gas affinity.

Mesoporous materials are also being used by Mitsubishi Heavy Industries, Ltd.[172] for a volatile organic compounds (VOC) recovery process. The high surface area of mesoporous aluminosilicates can be utilized to adsorb VOC at room temperature with great capacity. The saturated sorbent can be reactivated with hot air (120–150 °C) and the recovered VOC can be concentrated by 3–10 times. This process does not require the use of steam for adsorbent reactivation, and is flexible for recovery of various kinds of VOC. Izumi[172] has demonstrated that mesoporous materials can out-perform leading zeolite sorbents in the adsorption of methyl ethyl ketone by about twofold for a high SiO_2/Al_2O_3 ratio. The acidic, low-temperature synthesis developed also holds promise for the manufacture of mesoporous materials at a lower cost than high-silica zeolites.

For effective binding of heavy metals, Feng et al.[173] have functionalized the surface of mesoporous silicate supports with a monolayer of tris(methoxy)sulfanylpropylsilane molecules with thiol terminal groups. This strategy enabled mercury, silver, and lead ions to be proficiently adsorbed from tainted water so that the samples were rendered clean enough to drink. The adsorptive power of this new material was more than an order of magnitude higher than that of conventional sorbents. The sorbent was highly selective for certain metals; metal ions such as sodium, barium, and zinc were not taken up. It was also reusable; treatment of the mercury-loaded material with concentrated HCl would release the mercury, and the sorbent remained functional after multiple cycles. This example represented a powerful application of functionalized mesoporous materials as a selective sorbent with ultra-high surface activity.

4.5. Hosts for Quantum Structures

The well-defined mesoporous structure of M41S materials can be used as hosts for quantum semiconductor structures of low dimensionality. The cylindrical channels of the mesoporous structure of MCM-41 allow for matrix-mediated synthesis of molecular wires and quantum wires, and the silicate-based framework can provide electrical isolation of the conducting wires. Wu and Bein[174] have reported the adsorption of aniline and its polymerization in the pores of a transition metal containing mesoporous MCM-41 host. The resulting polyaniline filaments encapsulated in the 3 nm wide pore channels showed significant low-field conductivity, which indicated that they still supported mobile charge carriers.

Leon et al.[175] have demonstrated the feasibility of filling the mesopores with a semiconductor. Using vapor phase epitaxy, germanium filaments were deposited in the pore channels whereby surface hydroxyls acted as anchor points for seeding the nucleation of semiconductor clusters. The Ge crystallites took the shape and periodicity of the mesopores of the silicate matrix. While only some of the pores were filled and more complete semiconductor loading awaits future development, such fabrication techniques are promising towards generating quantum wire and dot arrays with high packing density.

For device fabrication, it would be of interest to derive the host inorganic materials in the form of thin films (instead of particulates), with ordered mesopores preferably oriented perpendicular to the plane of the films. It would also be important for many applications to achieve the quantum wires as continuous, single crystals.[176] This area of research holds a great deal of potential for significant technological impact, and may capitalize on the pore-size tunability of well-defined MCM-41 mesostructures for unique quantum confinement effects.

5. Summary and Outlook

The field of heterogeneous catalysis has benefited tremendously from the research in supramolecular-templated mesoporous materials and will continue to grow, especially with the development of materials of new compositions and surface modifications. The potential of mesoporous materials as catalysts has already been demonstrated in a number of areas, but only time will tell if these novel materials will find widespread commercial applications. Research in the preparation of materials that contain both surfactant-templated mesoporosity and controlled bulk features has just begun, and it remains to be seen if these systems can be developed for macrostructure-dependent applications, such as membrane separations. In spite of the large amount of synthesis work done already, relatively little research has been devoted to further elucidate the mechanisms of formation for the variety of mesostructures. Insights on self-assembly mechanisms will be useful towards expanding our capability to derive systematically tuned pore dimensions which span the microporous, mesoporous and macroporous regimes. Hierarchical mesostructures possessing patterned features on different length scales processed in the desired bulk morphologies also await further development as unique multifunctional devices.

Appendix

Abbreviations of mesoporous materials, proposed mechanisms, and substrates.

APM	acid-prepared mesostructures
CMC	critical micelle concentration
CTAB	cetyltrimethylammonium bromide
CTAC	cetyltrimethylammonium chloride

D4R	double four-ring
FSM	mesoporous materials prepared from kanemite
g	effective surfactant packing parameter
I	inorganic precursor
L_3	"sponge" mesopore phases
LAT	ligand-assisted templating
LC	liquid crystal
LCT	liquid crystal templating
M^+	metal cation
M41S	family of mesoporous materials
MCM-41	hexagonal mesoporous phase
MCM-48	cubic mesoporous phase
MCM-50	lamellar mesoporous phase
MOMS	mesoporous manganese oxides
MSU	mesoporous alumina phases
N^0	nonionic head group
S	surfactant head group
SBA	mesoporous materials derived by the APM method
SLC	silicatropic liquid crystal
TBOS	tetrabutylorthosilicate
TEOS	tetraethylorthosilicate
TMAOH	tetramethylammonium hydroxide
TMOS	tetramethylorthosilicate
TMS	mesoporous transition metal oxides (Tech molecular sieves)
X^-	counteranion

We acknowledge the financial support of the National Science Foundation and the David and Lucile Packard Foundation.

Received: December 1, 1997
Revised version: July 15, 1998 [A 262 IE]
German version: *Angew. Chem.* **1999**, *111*, 58 – 82

[1] a) C. T. Kresge, M. E. Leonowicz, W. J. Roth, J. C. Vartuli, J. S. Beck, *Nature* **1992**, *359*, 710 – 712; b) J. S. Beck, J. C. Vartuli, W. J. Roth, M. E. Leonowicz, C. T. Kresge, K. D. Schmitt, C. T.-W. Chu, D. H. Olsen, E. W. Sheppard, S. B. McCullen, J. B. Higgins, J. L. Schlenker, *J. Am. Chem. Soc.* **1992**, *114*, 10834 – 10843; c) C. T. Kresge, M. E. Leonowicz, W. J. Roth, J. C. Vartuli (Mobil Oil Corp.), US-A 5098684, **1992** [*Chem. Abstr.* **1992**, *117*, 72621].
[2] C. J. Brinker, *Curr. Opin. Solid State. Mater. Sci.* **1996**, *1*, 798 – 805.
[3] J. C. Vartuli, C. T. Kresge, W. J. Roth, S. B. McCullen, J. S. Beck, K. D. Schmitt, M. E. Leonowicz, J. D. Lutner, E. W. Sheppard in *Advanced Catalysts and Nanostructured Materials: Modern Synthesis Methods* (Ed.: W. R. Moser), Academic Press, New York, **1996**, pp. 1 – 19.
[4] G. D. Stucky, Q. Huo, A. Firouzi, B. F. Chmelka, S. Schacht, I. G. Voigt-Martin, F. Schüth in *Progress in Zeolite and Microporous Materials, Studies in Surface Science and Catalysis, Vol. 105* (Eds.: H. Chon, S.-K. Ihm, Y. S. Uh), Elsevier, Amsterdam, **1997**, pp. 3 – 28.
[5] N. K. Raman, M. T. Anderson, C. J. Brinker, *Chem. Mater.* **1996**, *8*, 1682 – 1701.
[6] D. M. Antonelli, J. Y. Ying, *Curr. Opin. Coll. Interf. Sci.* **1996**, *1*, 523 – 529.
[7] P. Behrens, *Angew. Chem.* **1996**, *108*, 561 – 564; *Angew. Chem. Int. Ed. Engl.* **1996**, *35*, 515 – 518.
[8] X. S. Zhao, G. Q. Lu, G. J. Millar, *Ind. Eng. Chem. Res.* **1996**, *35*, 2075 – 2090.
[9] A. Sayari, *Chem. Mater.* **1996**, *8*, 1840 – 1852.
[10] P. Behrens, *Adv. Mater.* **1993**, *5*, 127 – 132.
[11] J. S. Beck, J. C. Vartuli, G. J. Kennedy, C. T. Kresge, W. J. Roth, S. E. Schramm, *Chem. Mater.* **1994**, *6*, 1816 – 1821.
[12] J. C. Vartuli, C. T. Kresge, M. E. Leonowicz, A. S. Chu, S. B. McCullen, I. D. Johnson, E. W. Sheppard, *Chem. Mater.* **1994**, *6*, 2070 – 2077.
[13] C.-Y. Chen, S. L. Burkett, H.-X. Li, M. E. Davis, *Microporous Mater.* **1993**, *2*, 27 – 34.
[14] A. Steel, S. W. Carr, M. W. Anderson, *J. Chem. Soc. Chem. Commun.* **1994**, 1571 – 1572.
[15] A. Monnier, F. Schüth, Q. Huo, D. Kumar, D. Margolese, R. S. Maxwell, G. D. Stucky, M. Krishnamurty, P. Petroff, A. Firouzi, M. Janicke, B. F. Chmelka, *Science* **1993**, *261*, 1299 – 1303.
[16] G. D. Stucky, A. Monnier, F. Schüth, Q. Huo, D. Margolese, D. Kumar, M. Krishamurty, P. Petroff, A. Firouzi, M. Janicke, B. F. Chmelka, *Mol. Cryst. Liq. Cryst.* **1994**, *240*, 187 – 200.
[17] a) T. Yanagisawa, T. Shimizu, K. Kuroda, C. Kato, *Bull. Chem. Soc. Jpn.* **1990**, *63*, 988 – 992; b) S. Inagaki, Y. Fukushima, K. Kuroda, *J. Chem. Soc. Chem. Commun.* **1993**, 680 – 682; c) Y. Fukushima, S. Inagaki, *Mater. Sci. Eng. A* **1996**, *217 – 218*, 116 – 118.
[18] A. Firouzi, D. Kumar, L. M. Bull, T. Besier, P. Sieger, Q. Huo, S. A. Walker, J. A. Zasadzinski, C. Glinka, J. Nicol, D. Margolese, G. D. Stucky, B. F. Chmelka, *Science* **1995**, *267*, 1138 – 1143.
[19] S. Ikeda in *Surfactants in Solution, Vol. 2* (Eds.: K. L. Mittal, B. Lindman), Plenum, New York, **1984**, pp. 825 – 840.
[20] A. Firouzi, F. Atef, A. G. Oertli, G. D. Stucky, B. F. Chmelka, *J. Am. Chem. Soc.* **1997**, *119*, 3596 – 3610.
[21] C. A. Fyfe, G. Fu, *J. Am. Chem. Soc.* **1995**, *117*, 9709 – 9714.
[22] O. Regev, *Langmuir* **1996**, *12*, 4940 – 4944.
[23] a) Q. Huo, D. I. Margolese, U. Ciesla, P. Feng, T. E. Gier, P. Sieger, R. Leon, P. M. Petroff, F. Schüth, G. D. Stucky, *Nature* **1994**, *368*, 317 – 321; b) Q. Huo, D. I. Margolese, U. Ciesla, D. G. Demuth, P. Feng, T. E. Gier, P. Sieger, A. Firouzi, B. F. Chmelka, F. Schüth, G. D. Stucky, *Chem. Mater.* **1994**, *6*, 1176 – 1191.
[24] J. C. Vartuli, K. D. Schmitt, C. T. Kresge, W. J. Roth, M. E. Leonowicz, S. B. McCullen, S. D. Hellring, J. S. Beck, J. L. Schlenker, D. H. Olsen, E. W. Sheppard, *Chem. Mater.* **1994**, *6*, 2317 – 2326.
[25] J. C. Vartuli, C. T. Kresge, W. J. Roth, S. B. McCullen, J. S. Beck, K. D. Schmitt, M. E. Leonowicz, J. D. Lutner, E. W. Sheppard in *Proceedings of the 209th ACS National Meeting, Division of Petroleum Chemistry* **1995**, pp. 21 – 25.
[26] Q. Huo, D. I. Margolese, G. D. Stucky, *Chem. Mater.* **1996**, *8*, 1147 – 1160.
[27] V. Luzzati, R. Vargas, P. Mariani, A. Gulik, H. Delacroix, *J. Mol. Biol.* **1993**, *229*, 540 – 551.
[28] J. N. Israelachvili, *Intermolecular and Surface Forces*, 2nd ed., Academic Press, London, **1992**, pp. 366 – 394.
[29] Q. Huo, R. Leon, P. M. Petroff, G. D. Stucky, *Science* **1995**, *268*, 1324 – 1327.
[30] a) J. M. Kim, S. K. Kim, R. Ryoo, *Chem. Commun.* **1998**, 259 – 260; b) K. W. Gallis, C. C. Landry, *Chem. Mater.* **1997**, *9*, 2035 – 2038.
[31] F. Chen, L. Huang, Q. Li, *Chem. Mater.* **1997**, *9*, 2685 – 2686.
[32] P. T. Tanev, T. J. Pinnavaia, *Science* **1995**, *267*, 865 – 867.
[33] P. T. Tanev, T. J. Pinnavaia, *Chem. Mater.* **1996**, *8*, 2068 – 2079.
[34] P. T. Tanev, T. J. Pinnavaia, *Science* **1996**, *271*, 1267 – 1269.
[35] S. A. Bagshaw, E. Prouzet, T. J. Pinnavaia, *Science* **1995**, *269*, 1242 – 1244.
[36] G. S. Attard, J. C. Glyde, C. G. Göltner, *Nature* **1995**, *378*, 366 – 368.
[37] a) C. G. Göltner, M. Antonietti, *Adv. Mater.* **1997**, *9*, 431 – 436; b) C. G. Göltner, S. Henke, M. C. Weissenberger, M. Antonietti, *Angew. Chem.* **1998**, *110*, 633 – 636; *Angew. Chem. Int. Ed.* **1998**, *37*, 613 – 616.
[38] K. M. McGrath, D. M. Dabbs, N. Yao, I. A. Aksay, S. M. Gruner, *Science* **1997**, *277*, 552 – 556.
[39] a) R. Ryoo, J. M. Kim, C. H. Ko, C. H. Shin, *J. Phys. Chem.* **1996**, *100*, 17718 – 17721; b) R. Ryoo, J. M. Kim, C. H. Shin, J. Y. Lee in *Progress in Zeolite and Microporous Materials, Studies in Surface Science and Catalysis, Vol. 105* (Eds.: H. Chon, S.-K. Ihm, Y. S. Uh), Elsevier, Amsterdam, **1997**, pp. 45 – 52.
[40] R. Ryoo, C. H. Ko, R. F. Howe, *Chem. Mater.* **1997**, *9*, 1607 – 1613.
[41] A. Corma, M. T. Navarro, J. Pérez Pariente, *J. Chem. Soc. Chem. Commun.* **1994**, 147 – 148.
[42] K. M. Reddy, I. Moudrakovski, A. Sayari, *J. Chem. Soc. Chem. Commun.* **1994**, 1059 – 1060.
[43] P. T. Tanev, M. Chibwe, T. J. Pinnavaia, *Nature* **1994**, *368*, 321 – 323.
[44] A. Sayari, C. Danumah, I. L. Moudrakovski, *Chem. Mater.* **1995**, *7*, 813 – 815.

[45] Z. Luan, C.-F. Cheng, W. Zhou, J. Klinowski, *J. Phys. Chem.* **1995**, *99*, 1018 – 1024.
[46] G. Fu, C. A. Fyfe, W. Schwieger, G. T. Kokotailo, *Angew. Chem.* **1995**, *107*, 1582 – 1585; *Angew. Chem. Int. Ed. Engl.* **1995**, *34*, 1499 – 1502.
[47] D. Zhao, D. Goldfarb, *J. Chem. Soc. Chem. Commun.* **1995**, 875 – 876.
[48] T. M. Abdel-Fattah, T. J. Pinnavaia, *Chem. Commun.* **1996**, 665 – 666.
[49] C.-F. Cheng, H. He, W. Zhou, J. Klinowski, J. A. S. Gonçalves, L. F. Gladden, *J. Phys. Chem.* **1996**, *100*, 390 – 396.
[50] C.-F. Cheng, J. Klinowski, *J. Chem. Soc. Faraday Trans.* **1996**, *92*, 289 – 292.
[51] K. A. Koyano, T. Tatsumi, *Chem. Commun.* **1996**, 145 – 146.
[52] A. Tuel, S. Gontier, *Chem. Mater.* **1996**, *8*, 114 – 122.
[53] A. Tuel, S. Gontier, R. Teissier, *Chem. Commun.* **1996**, 651 – 652.
[54] N. Ulagappan, C. N. R. Rao, *Chem. Commun.* **1996**, 1047 – 1048.
[55] W. Zhang, T. J. Pinnavaia, *Catal. Lett.* **1996**, *38*, 261 – 265.
[56] W. Zhang, J. Wang, P. T. Tanev, T. J. Pinnavaia, *Chem. Commun.* **1996**, 979 – 980.
[57] B. Echchahed, A. Moen, D. Nicholson, L. Bonneviot, *Chem. Mater.* **1997**, *9*, 1716 – 1719.
[58] N.-Y. He, J.-M. Cao, S.-L. Bao, Q.-H. Xu, *Mater. Lett.* **1997**, *31*, 133 – 136.
[59] D. J. Jones, J. Jiménez-Jiménez, A. Jiménez-López, P. Maireles-Torres, P. Olivera-Pastor, E. Rodriguez-Castellón, J. Rozière, *Chem. Commun.* **1997**, 431 – 432.
[60] L. Zhang, J. Y. Ying, *AIChE J.* **1997**, *43*, 2793 – 2801.
[61] M. S. Wong, H. C. Huang, J. Y. Ying, unpublished results.
[62] U. Ciesla, D. Demuth, R. Leon, P. Petroff, G. Stucky, K. Unger, F. Schüth, *J. Chem. Soc. Chem. Commun.* **1994**, 1387 – 1388.
[63] D. M. Antonelli, J. Y. Ying, *Angew. Chem.* **1995**, *107*, 2202 – 2206; *Angew. Chem. Int. Ed. Engl.* **1995**, *34*, 2014 – 2017.
[64] D. M. Antonelli, J. Y. Ying, *Angew. Chem.* **1996**, *108*, 461 – 464; *Angew. Chem. Int. Ed. Engl.* **1996**, *35*, 426 – 430.
[65] D. M. Antonelli, A. Nakahira, J. Y. Ying, *Inorg. Chem.* **1996**, *35*, 3126 – 3136.
[66] D. M. Antonelli, J. Y. Ying, *Chem. Mater.* **1996**, *8*, 874 – 881.
[67] M. S. Wong, D. M. Antonelli, J. Y. Ying, *Nanostr. Mater.* **1997**, *9*, 165 – 168.
[68] M. S. Wong, J. Y. Ying, *Chem. Mater.* **1998**, *10*, 2067 – 2077
[69] A. Stein, M. Fendorf, T. P. Jarvie, K. T. Mueller, A. J. Benesi, T. E. Mallouk, *Chem. Mater.* **1995**, *7*, 304 – 313.
[70] G. G. Janauer, A. Dobley, J. Guo, P. Zavalij, M. S. Whittingham, *Chem. Mater.* **1996**, *8*, 2096 – 2101.
[71] a) V. Luca, D. J. MacLachlan, J. M. Hook, R. Withers, *Chem. Mater.* **1995**, *7*, 2220 – 2223; b) V. Luca, J. M. Hook, *Chem. Mater.* **1997**, *9*, 2731 – 2744.
[72] J. Luo, S. L. Suib, *Chem. Commun.* **1997**, 1031 – 1032.
[73] Z.-R. Tian, W. Tong, J.-Y. Wang, N.-G. Duan, V. V. Krishnan, S. L. Suib, *Science* **1997**, *276*, 926 – 930.
[74] S. A. Bagshaw, T. J. Pinnavaia, *Angew. Chem.* **1996**, *108*, 1180 – 1183; *Angew. Chem. Int. Ed. Engl.* **1996**, *35*, 1102 – 1105.
[75] F. Vaudry, S. Khodabandeh, M. E. Davis, *Chem. Mater.* **1996**, *8*, 1451 – 1464.
[76] M. Yada, M. Machida, T. Kijima, *Chem. Commun.* **1996**, 769 – 770.
[77] A. Sayari, I. Moudrakovski, J. S. Reddy, C. I. Ratcliffe, J. A. Ripmeester, K. F. Preston, *Chem. Mater.* **1996**, *8*, 2080 – 2088.
[78] A. Sayari, V. R. Karra, J. S. Reddy, I. L. Moudrakovski, *J. Chem. Soc. Chem. Commun.* **1996**, 411 – 412.
[79] A. Chenite, Y. Le Page, V. R. Karra, A. Sayari, *J. Chem. Soc. Chem. Commun.* **1996**, 413 – 414.
[80] S. Oliver, A. Kuperman, N. Coombs, A. Lough, G. A. Ozin, *Nature* **1995**, *378*, 47 – 50.
[81] P. Feng, Y. Xia, J. Feng, X. Bu, G. D. Stucky, *Chem. Commun.* **1997**, 949 – 950.
[82] D. Zhao, Z. Luan, L. Kevan, *Chem. Commun.* **1997**, 1009 – 1010.
[83] B. Chakraborty, A. C. Pulikottil, S. Das, B. Viswanathan, *Chem. Commun.* **1997**, 911 – 912.
[84] T. Abe, A. Taguchi, M. Iwamoto, *Chem. Mater.* **1995**, *7*, 1429 – 1430.
[85] T. Doi, T. Miyake, *Chem. Commun.* **1996**, 1635 – 1636.
[86] M. J. Hudson, J. A. Knowles, *J. Mater. Chem.* **1996**, *6*, 89 – 95.
[87] J. S. Reddy, A. Sayari, *Catal. Lett.* **1996**, *38*, 219 – 223.
[88] U. Ciesla, S. Schacht, G. D. Stucky, K. K. Unger, F. Schüth, *Angew. Chem.* **1996**, *108*, 597 – 600; *Angew. Chem. Int. Ed. Engl.* **1996**, *35*, 541 – 543.
[89] P. Liu, J. S. Reddy, A. Adnot, A. Sayari, *Mater. Res. Soc. Symp. Proc.* **1996**, *431*, 101 – 106.
[90] P. Liu, J. Liu, A. Sayari, *Chem. Commun.* **1997**, 577 – 578.
[91] a) P. V. Braun, P. Osenar, S. I. Stupp, *Nature* **1996**, *380*, 325 – 328; b) V. Tohver, P. V. Braun, M. U. Pralle, S. I. Stupp, *Chem. Mater.* **1997**, *9*, 1495 – 1498.
[92] J. Li, L. Delmotte, H. Kessler, *Chem. Commun.* **1996**, 1023 – 1024.
[93] D. Zhao, D. Goldfarb, *Chem. Mater.* **1996**, *8*, 2571 – 2578.
[94] G. S. Attard, C. G. Göltner, J. M. Corker, S. Henke, R. H. Templer, *Angew. Chem.* **1997**, *109*, 1372 – 1374; *Angew. Chem. Int. Ed. Engl.* **1997**, *36*, 1315 – 1317.
[95] A. Navrotsky, I. Petrovic, Y. Hu, C.-Y. Chen, M. E. Davis, *J. Non-Cryst. Solids* **1995**, *192&193*, 474 – 477.
[96] T. Sun, J. Y. Ying, *Nature* **1997**, *389*, 704 – 706.
[97] T. Sun, J. Y. Ying, *Angew. Chem.* **1998**, *110*, 690 – 693; *Angew. Chem. Int. Ed.* **1998**, *37*, 664 – 667.
[98] D. Zhao, J. Feng, Q. Huo, N. Melosh, G. H. Fredrickson, B. F. Chmelka, G. D. Stucky, *Science* **1998**, *279*, 548 – 552.
[99] I. W. C. E. Arends, R. A. Sheldon, M. Wallau, U. Schuchardt, *Angew. Chem.* **1997**, *109*, 1190 – 1211; *Angew. Chem. Int. Ed. Engl.* **1997**, *36*, 1144 – 1163.
[100] J. S. Reddy, A. Sayari, *J. Chem. Soc. Chem. Commun.* **1995**, 2231 – 2232.
[101] S. Gontier, A. Tuel, *J. Catal.* **1995**, *157*, 124 – 132.
[102] I. Vankelecom, K. Vercruysse, N. Moens, R. Parton, J. S. Reddy, P. Jacobs, *Chem. Commun.* **1997**, 137 – 138.
[103] A. Corma, A. Martinez, V. Martinez-Soria, J. B. Monton, *J. Catal.* **1995**, *153*, 25 – 31.
[104] K. M. Reddy, C. Song, *Catal. Lett.* **1996**, *36*, 103 – 109.
[105] K. M. Reddy, C. Song, *Catal. Today* **1996**, *31*, 137 – 144.
[106] B. A. Aufdembrink, A. W. Chester, J. A. Herbst, C. T. Kresge (Mobil Oil Corp.), US-A 5258114, **1993** [*Chem. Abstr.* **1991**, *115*,-139158].
[107] J. S. Beck, D. C. Calabro, S. B. McCullen, B. P. Pelrine, K. D. Schmitt, J. C. Vartuli (Mobil Oil Corp.), US-A 5200058, **1993** [*Chem. Abstr.* **1991**, *115*, 139158].
[108] N. A. Bhore, Q. N. Le, G. H. Yokomizo (Mobil Oil Corp.), US-A 5134243, **1992** [*Chem. Abstr.* **1993**, *118*, 106144].
[109] Q. N. Le, R. T. Thomson, G. H. Yokomizo (Mobil Oil Corp.), US-A 5134241, **1992** [*Chem. Abstr.* **1992**, *117*, 237023].
[110] Q. N. Le, R. T. Thomson, G. H. Yokomizo (Mobil Oil Corp.), US-A 5134242, **1992** [*Chem. Abstr.* **1993**, *118*, 172297].
[111] Q. N. Le, R. T. Thomson (Mobil Oil Corp.), US-A 5232580, **1993** [*Chem. Abstr.* **1993**, *119*, 52652].
[112] Q. N. Le, R. T. Thomson (Mobil Oil Corp.), US-A 5191144, **1993** [*Chem. Abstr.* **1993**, *119*, 31334].
[113] T. F. Degnan, Jr., K. M. Keville, D. O. Marler, D. N. Mazzone (Mobil Oil Corp.), US-A 5281328, **1994** [*Chem. Abstr.* **1993**, *119*, 31376].
[114] M. R. Apelian, T. F. Degnan, Jr., D. O. Marler, D. N. Mazzone (Mobil Oil Corp.), US-A 5227353, **1993** [*Chem. Abstr.* **1993**, *119*, 31331].
[115] M. R. Apelian, T. F. Degnan, Jr., D. O. Marler, D. N. Mazzone (Mobil Oil Corp.), US-A 5264116, **1993** [*Chem. Abstr.* **1993**, *119*, 31355].
[116] T. F. Degnan, Jr., K. M. Keville, M. E. Landis, D. O. Marler, D. N. Mazzone (Mobil Oil Corp.), US-A 5183557, **1993** [*Chem. Abstr.* **1993**, *119*, 31376].
[117] T. F. Degnan, Jr., K. M. Keville, M. E. Landis, D. O. Marler, D. N. Mazzone (Mobil Oil Corp.), US-A 5290744, **1994** [*Chem. Abstr.* **1993**, *119*, 31376].
[118] D. O. Marler, D. N. Mazzone (Mobil Oil Corp.), US-A 5288395, **1994** [*Chem. Abstr.* **1993**, *119*, 31354].
[119] D. O. Marler, D. N. Mazzone (Mobil Oil Corp.), US-A 5277792, **1994** [*Chem. Abstr.* **1993**, *119*, 31355].
[120] J. Aguado, D. P. Serrano, M. D. Romero, J. M. Escola, *Chem. Commun.* **1996**, 725 – 726.
[121] M. J. Climent, A. Corma, S. Iborra, M. C. Navarro, J. Primo, *J. Catal.* **1996**, *161*, 783 – 789.
[122] K. R. Kloetstra, H. van Bekkum, *J. Chem. Res.* **1995**, 26 – 27.
[123] E. Armengol, M. L. Cano, A. Corma, H. Garcia, M. T. Navarro, *J. Chem. Soc. Chem. Commun.* **1995**, 519 – 520.
[124] Q. N. Le (Mobil Oil Corp.), US-A 5191134, **1993** [*Chem. Abstr.* **1993**, *118*, 212647].

[125] T. F. Degnan, Jr., K. J. Del Rossi, A. Huss, Jr. (Mobil Oil Corp.), US-A 5191148, **1993** [*Chem. Abstr.* **1993**, *118*, 256987].
[126] T. F. Degnan, Jr., K. J. Del Rossi, A. Husain, A. Huss, Jr., US-A 5191147, **1993** [*Chem. Abstr.* **1993**, *119*, 163816].
[127] Q. N. Le (Mobil Oil Corp.), US-A 5118894, **1992** [*Chem. Abstr.* **1992**, *117*, 153192].
[128] A. Corma, M. Iglesias, F. Sanchez, *J. Chem. Soc. Chem. Commun.* **1995**, 1635 – 1636.
[129] J. S. Beck, R. F. Socha, D. S. Shihiba, J. C. Vartuli (Mobil Oil Corp.), US-A 5143707, **1992** [*Chem. Abstr.* **1993**, *118*, 26784].
[130] C. T. Kresge, M. E. Leonowicz, W. J. Roth, J. C. Vartuli, K. M. Keville, S. S. Shih, T. F. Degnan, Jr., F. G. Dwyer, M. E. Landis (Mobil Oil Corp.), US-A 5183561, **1993** [*Chem. Abstr.* **1991**, *115*, 139158].
[131] B. P. Pelrine, K. D. Schmitt, J. C. Vartuli (Mobil Oil Corp.), US-A 5105051, **1992** [*Chem. Abstr.* **1992**, *117*, 154327].
[132] B. P. Pelrine, K. D. Schmitt, J. C. Vartuli (Mobil Oil Corp.), US-A 5270273, **1993** [*Chem. Abstr.* **1994**, *120*, 303101].
[133] N. A. Bhore, I. D. Johnson, K. M. Keville, Q. N. Le, G. H. Yokomizo (Mobil Oil Corp.), US-A 5260501, **1993** [*Chem. Abstr.* **1992**, *117*, 237023].
[134] K. J. Del Rossi, G. H. Hatzikos, A. Huss, Jr. (Mobil Oil Corp.), US-A 5256277, **1993** [*Chem. Abstr.* **1993**, *119*, 31332].
[135] W. S. Borghard, C. T. Chu, T. F. Degnan, Jr., S. S. Shih (Mobil Oil Corp.), US-A 5264641, **1993** [*Chem. Abstr.* **1994**, *120*, 133915].
[136] C. T. Kresge, D. O. Marler, G. S. Rav, B. H. Rose (Mobil Oil Corp.), US-A 5366945, **1994** [*Chem. Abstr.* **1995**, *122*, 110416].
[137] K. R. Kloetstra, H. van Bekkum, *J. Chem. Soc. Chem. Commun.* **1995**, 1005 – 1006.
[138] T. Maschmeyer, F. Rey, G. Sankar, J. M. Thomas, *Nature* **1995**, *378*, 159 – 162.
[139] R. Neumann, A. M. Khenkin, *Chem. Commun.* **1996**, 2643 – 2644.
[140] R. Burch, N. Cruise, D. Gleeson, S. C. Tsang, *Chem. Commun.* **1996**, 951 – 952.
[141] J. Y. Ying, C. P. Mehnert (Massachusetts Institute of Technology), US Patent pending, **1997**.
[142] C. P. Mehnert, J. Y. Ying, *Chem. Commun.* **1997**, 2215 – 2216.
[143] C. P. Mehnert, D. Weaver, J. Y. Ying, *J. Am. Chem. Soc.*, in press.
[144] C. Liu, X. Ye, Y. Wu, *Catal. Lett.* **1996**, *36*, 263 – 266.
[145] P. Sutra, D. Brunel, *Chem. Commun.* **1996**, 2485 – 2486.
[146] Y. V. S. Rao, D. E. De Vos, T. Bein, P. A. Jacobs, *Chem. Commun.* **1997**, 355 – 356.
[147] J. F. Diaz, K. J. Balkus, Jr., F. Bedioui, V. Kurshev, L. Kevan, *Chem. Mater.* **1997**, *9*, 61 – 67.
[148] N. Herron, G. D. Stucky, C. A. Tolman, *J. Chem. Soc. Chem. Commun.* **1986**, 1521 – 1522.
[149] N. Herron, *Inorg. Chem.* **1986**, *25*, 4714 – 4723.
[150] C.-J. Liu, S.-G. Li, W.-Q. Pang, C.-M. Che, *Chem. Commun.* **1997**, 65 – 66.
[151] L. Zhang, T. Sun, J. Y. Ying, **1997**, unpublished results.
[152] S. O'Brien, J. Tudor, S. Barlow, M. J. Drewitt, S. J. Heyes, D. O'Hare, *Chem. Commun.* **1997**, 641 – 642.
[153] T. Maschmeyer, R. D. Oldroyd, G. Sankar, J. M. Thomas, I. J. Shannon, J. A. Klepetko, A. F. Masters, J. K. Beattie, C. R. A. Catlow, *Angew. Chem.* **1997**, *109*, 1713 – 1716; *Angew. Chem. Int. Ed. Engl.* **1997**, *36*, 1639 – 1642.
[154] Y. S. Ko, T. K. Han, J. W. Park, S. I. Woo, *Macromol. Rapid Commun.* **1996**, *17*, 749 – 750.
[155] J. Tudor, D. O'Hare, *Chem. Commun.* **1997**, 603 – 604.
[156] C. P. Mehnert, B. L. Lungwitz, D. Seyferth, J. Y. Ying, **1997**, unpublished results.
[157] H. Yang, A. Kuperman, N. Coombs, S. Mamiche-Afara, G. A. Ozin, *Nature* **1996**, *379*, 703 – 705.
[158] H. Yang, N. Coombs, I. Sokolov, G. A. Ozin, *Nature* **1996**, *381*, 589 – 592.
[159] I. Aksay, M. Trau, S. Manne, I. Honma, N. Yao, L. Zhou, P. Fenter, P. M. Eisenberger, S. M. Gruner, *Science* **1996**, *273*, 892 – 898.
[160] M. Ogawa, *Chem. Commun.* **1996**, 1149 – 1150.
[161] W. Hillhouse, T. Okubo, J. W. van Egmond, M. Tsapatsis, *Chem. Mater.* **1997**, *9*, 1505 – 1507.
[162] S. H. Tolbert, A. Firouzi, G. D. Stucky, B. F. Chmelka, *Science* **1997**, *278*, 264 – 268.
[163] Y. Lu, R. Ganguli, C. A. Drewien, M. T. Anderson, C. J. Brinker, W. Gong, Y. Guo, H. Soyez, B. Dunn, M. H. Huang, J. I. Zink, *Nature* **1997**, *389*, 364 – 368.
[164] S. H. Tolbert, T. E. Schäffer, J. Feng, P. K. Hansma, G. D. Stucky, *Chem. Mater.* **1997**, *9*, 1962 – 1967.
[165] H.-P. Lin, C.-Y. Mou, *Science* **1996**, *273*, 765 – 768.
[166] Q. Huo, J. Feng, F. Schüth, G. D. Stucky, *Chem. Mater.* **1997**, *9*, 14 – 17.
[167] S. Schacht, Q. Huo, G. Voigt-Martin, G. D. Stucky, F. Schüth, *Science* **1996**, *273*, 768 – 771.
[168] a) H. Yang, N. Coombs, G. A. Ozin, *Nature* **1997**, *386*, 692 – 695; b) G. A. Ozin, H. Yang, I. Sokolov, N. Coombs, *Adv. Mater.* **1997**, *9*, 662 – 667.
[169] S. A. Davis, S. L. Burkett, N. H. Mendelson, S. Mann, *Nature* **1997**, *385*, 420 – 423.
[170] A. Galarneau, A. Barodawalla, T. J. Pinnavaia, *Nature* **1995**, *374*, 529 – 531.
[171] M. A. Ioneva, G. K. Newman, J. H. Harwell, *AIChE Symp. Ser.* **1995**, *91*(309), 40 – 48.
[172] J. Izumi, *Mitsubishi VOC Recovery Process*, Mitsubishi Heavy Industries, Ltd., **1996**.
[173] a) X. Feng, G. E. Fryxell, L.-Q. Wang, A. Y. Kim, J. Liu, K. M. Kemner, *Science* **1997**, *276*, 923 – 926; b) J. Liu, X. Feng, G. E. Fryxell, L.-Q. Wang, A. Y. Kim, M. Gong, *Adv. Mater.* **1998**, *10*, 161 – 165.
[174] C.-G. Wu, T. Bein, *Chem. Mater.* **1994**, *6*, 1109 – 1112.
[175] R. Leon, D. Margolese, G. Stucky, P. M. Petroff, *Phys. Rev. B* **1995**, *52*, 2285 – 2288.
[176] Z. Zhang, J. Y. Ying, M. S. Dresselhaus, *J. Mater. Res.* **1998**, *13*, 1745 – 1748.